



IEEE
Power & Energy Society[®]

PowerTech Belgrade 2023

LEADING INNOVATIONS FOR RESILIENT
& CARBON-NEUTRAL POWER SYSTEMS
25-29 JUNE, 2023, BELGRADE, SERBIA

Harmonic Power-Flow Study of Converter-Dominated Grids

Speakers: Prof. Mario Paolone
Johanna Becker

Part 1 – Theory

1. Motivation & Problem Statement
2. Primer on Linear Time-Periodic Systems and Toeplitz Matrices
3. Harmonic Power-Flow Modelling Framework
4. Solution Algorithm

Part 2 – CIDER Models, Code & Examples

1. Detailed CIDER Models
2. Code Structure
3. Validation & Demonstration

Tutorial slides and code available on:



<https://github.com/DESL-EPFL/Harmonic-Power-Flow-Method>

Part 1 - Theory

- Power distribution grids are experiencing a massive integration of Distributed Energy Resources (DERs).
- Evolution towards Active Distribution Networks (ADNs)
 - Power systems whose controllability is enabled by power electronic interfaces of the DERs.
- DERs are mostly Converter-Interface Distributed Energy Resources (CIDERs).
 - Increasing number of CIDERs impacts power quality of ADNs.
 - Interactions between different CIDERs through the grid can lead to undesirable amplifications at harmonic frequencies → Harmonic instability.
 - Need for tools that accurately analyse the coupling and propagation of those harmonics.

Harmonic Instability

Definition [1]: Harmonic instability is a control-system stability issue due to:

- Inadequate control schemes (e.g., harmonic resonance of parallel DERs)
- Poor tuning of one or more equipment controllers.

➤ The system cannot be stabilized until the said controller(s) is retuned or the associated piece of equipment is disconnected.

- Phenomenon was observed:
 - In power transmission systems with HVDC links [2].
 - In power distribution systems with high share of CIDERs [3].

Classification of Harmonic Analysis Tools:

- Harmonic analysis tools can be clustered into:
 - i. Transient.
 - ii. Steady-state.
 - iii. Hybrid methods.

Classification of Harmonic Analysis Tools:

- Harmonic analysis tools can be clustered into:
 - i. Transient.
 - ii. Steady-state.
 - iii. Hybrid methods.
- Transient methods work with time-domain models (i.e., compute steady state via time-domain simulations and do a DFT on the obtained waveforms).
 - Classical nodal analysis (e.g., EMTP [4])
 - Modified Nodal Analysis (MNA, e.g., SPICE [5])
 - Modified Augmented Nodal Analysis (MANA, e.g., EMTP-RV [6]).
 - Accurate, but computationally intensive.
 - Impractical for the analysis of large systems.

Classification of Harmonic Analysis Tools:

- Harmonic analysis tools can be clustered into:
 - i. Transient.
 - ii. Steady-state.
 - iii. Hybrid methods.
- Steady-state methods work with frequency-domain models (i.e., system steady-state equilibrium is directly computed for each frequency).
 - *Direct Harmonic Analysis* (DHA): Harmonic frequencies are inferred through approximated linear functions from standard power-flow solution at fundamental frequency (e.g., [7]).
 - *Iterative Harmonic Analysis* (IHA) or *Harmonic Power-Flow* (HPF) study: iterative solution of the nonlinear HPF equations (e.g., [8]).
 - Simplified HPF (standard approach): Each frequency considered separately.
 - Sophisticated HPF: The coupling between harmonics is explicitly considered.
- Computationally more efficient than transient methods.
- Reliability of results relies on the accuracy of the underlying models.

Classification of Harmonic Analysis Tools:

- Harmonic analysis tools can be clustered into:
 - i. Transient.
 - ii. Steady-state.
 - iii. Hybrid methods.
- Hybrid methods are a combination of transient and steady-state methods:
 - Only a few strongly nonlinear elements are treated in time domain [9,10].
 - Computationally more efficient than pure transient methods.

- Steady-state methods appear to be promising in terms of computational complexity.
- Main challenge: Underlying models need to be accurate, computationally efficient and generally applicable at the same time.
- Most of the existing frequency-domain methods are valid only for specific devices and controllers or neglect the coupling between harmonics.
- A recent HPF Method combines the following features [11,12]:
 - Modularity w.r.t. the resource components.
 - Genericness w.r.t. the controls laws (i.e., grid-forming & -following behaviour).
 - Accuracy w.r.t. the generation and propagation of harmonics (in particular, the coupling between different harmonics).

Harmonic Power-Flow Method:

HPF framework employs Linear Time-Periodic (LTP) systems theory [13]:

- LTP systems can be employed for the analysis of CIDERS [14,15].
 - LTP systems are a generalization of LTI systems, where matrices can be time-periodic instead of time-invariant.
- For the HPF study, the LTP state-space models are developed in time domain.
- Then described in frequency domain by Toeplitz matrices composed of Fourier coefficients.

Linear Time-Periodic (LTP) Systems:

- Definition of an LTP system (all quantities are time-periodic w.r.t. the period $T = \frac{1}{f_1}$, f_1 being the fundamental frequency).
- The time-domain quantities can be represented by their Fourier Series:
 - Where $\mathbf{x}_h \in \mathbb{C}$ describes the Fourier coefficient of the h th harmonic.
 - With $h \in \mathcal{H} \subset \mathbb{Z}$ being the harmonic orders.
- In order for $\mathbf{x}(t)$ to be real-valued, the positive and negative spectrum have to be complex conjugates of each other.
- The multiplication of two quantities in time domain results in a convolution in frequency domain.

$$\dot{\mathbf{x}}(t) = \mathbf{A}(t)\mathbf{x}(t) + \mathbf{B}(t)\mathbf{u}(t)$$

$$\mathbf{y}(t) = \mathbf{C}(t)\mathbf{x}(t) + \mathbf{D}(t)\mathbf{u}(t)$$

$$\mathbf{x}(t) = \sum_{h \in \mathcal{H}} \mathbf{x}_h \exp(j h 2\pi f_1 t)$$

$$\mathbf{x}_{|h|} = \mathbf{x}_{-|h|}^*$$

$$\mathbf{A}(t)\mathbf{x}(t) \leftrightarrow \mathbf{A}(f) \odot \mathbf{X}(f)$$

Toeplitz Matrices:

- Structure of a $n \times n$ Toeplitz matrix $\hat{\mathbf{M}}$:

$$\hat{\mathbf{M}} = \begin{bmatrix} a & g & h & i & j \\ b & a & g & h & i \\ c & b & a & g & h \\ d & c & b & a & g \\ e & d & c & b & a \end{bmatrix}$$

- The convolution $\mathbf{A}(f) \odot \mathbf{X}(f)$ is then given by [13]:

- where $\hat{\mathbf{A}}$ is a Toeplitz matrix of the Fourier coefficients \mathbf{A}_h
- and $\hat{\mathbf{X}}$ is the column vector of the Fourier coefficients \mathbf{X}_h .

$$\mathbf{A}(t)\mathbf{x}(t) \leftrightarrow \mathbf{A}(f) \odot \mathbf{X}(f) = \hat{\mathbf{A}}\hat{\mathbf{X}}$$

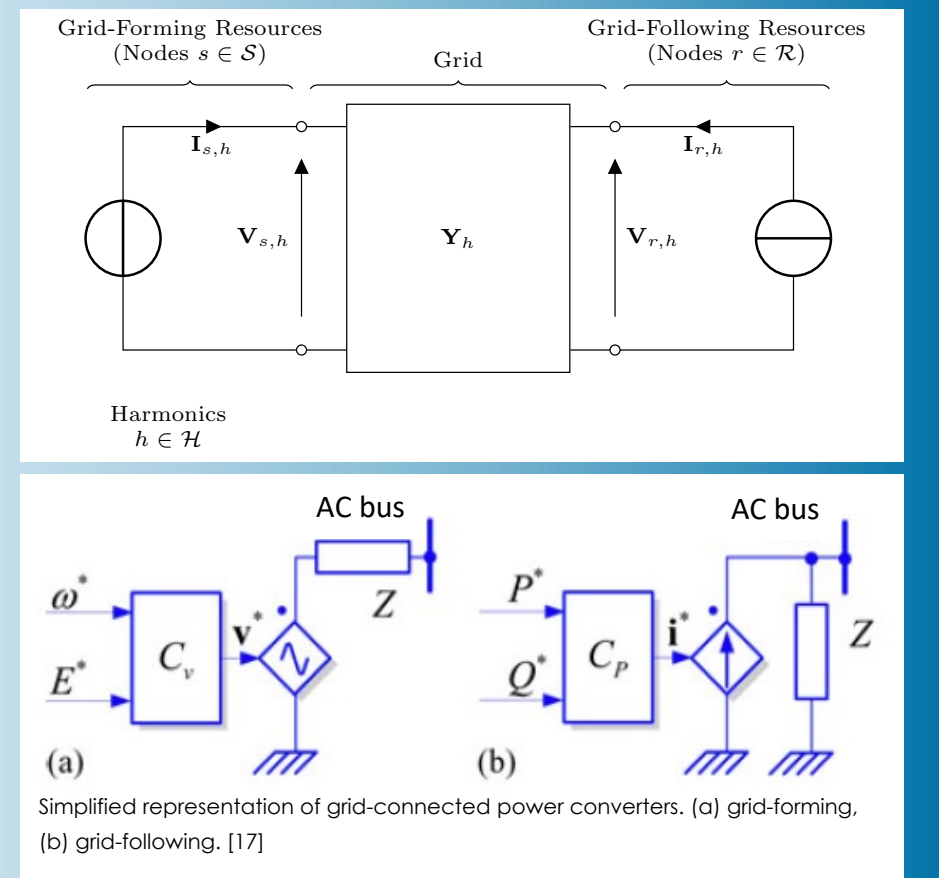
$$\begin{aligned} \hat{\mathbf{A}}: \hat{\mathbf{A}}_{mn} &= \mathbf{A}_h, m, n \in \mathbb{N}, h = m - n \in \mathcal{H} \\ \hat{\mathbf{X}} &= \text{col}_{h \in \mathcal{H}}(\mathbf{X}_h) \end{aligned}$$

- Such matrices and vectors are of infinite size.
 - In practice, only harmonics up to the maximum order h_{max} are considered.
- Coupling between harmonics of different order is represented by off-diagonals in the Toeplitz matrix.

$$\hat{\mathbf{A}}\hat{\mathbf{X}} = \begin{bmatrix} \ddots & \ddots & & & \\ & \mathbf{A}_0 & \mathbf{A}_{-1} & & \\ & \mathbf{A}_1 & \mathbf{A}_0 & \mathbf{A}_{-1} & \\ & & \mathbf{A}_1 & \mathbf{A}_0 & \ddots \\ & & & & \ddots \end{bmatrix} \begin{bmatrix} \mathbf{X}_{-1} \\ \mathbf{X}_0 \\ \mathbf{X}_1 \\ \vdots \end{bmatrix}$$

System Structure:

- The power system consists of the grid and resources.
- Grid:
Represented by hybrid parameters derived from its admittance matrix.
- Resource behaviour [16]:
 - Grid-forming: Controls magnitude and angle of the voltage at the PCC.
 - Grid-following: Injected currents are controlled with a specific phase displacement with respect to the grid voltage at the PCC.
 - Fundamental frequency phasor of the grid voltage at the PCC has to be known at any time for the correct calculation of the converter reference currents.
- The set of all nodes is described by $n \in \mathcal{N}$.
- They are further partitioned as $\mathcal{N} = \mathcal{S} \cup \mathcal{R}, \mathcal{S} \cap \mathcal{R} = \emptyset$, where \mathcal{S} and \mathcal{R} are the points of connection of grid-forming and grid-following resources, respectively.

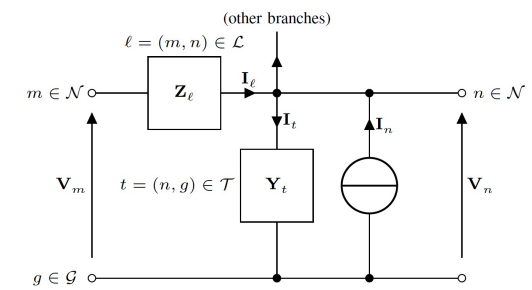


Grid Model – Branch and Shunt Elements:

- Grid is represented by a set of lumped-element models, that are linear and passive.
- Branch element $\ell \in \mathcal{L}$:
- Shunt element $t \in \mathcal{T}$:

$n \in \mathcal{N}$: The nodes.
 $g \in \mathcal{G}$: The ground.
 $\ell \in \mathcal{L}$: The branches.
 $t \in \mathcal{T}$: The shunt elements.

The lumped element model:



$$\mathbf{V}_m(f) - \mathbf{V}_n(f) = \mathbf{Z}_\ell(f)\mathbf{I}_\ell(f) \quad \forall \ell = (m, n) \in \mathcal{L}$$

$$\mathbf{I}_t(f) = \mathbf{Y}_t(f)\mathbf{V}_n(f) \quad \forall t = (n, g) \in \mathcal{T}$$

Model can represent generic three-phase grids with:

- Radial or meshed topology.
- Transposed or non-transposed lines.
- Balanced or unbalanced nodal injections.

Grid Model – Compound Admittance Matrix:

- The branch graph $\mathfrak{B} := (\mathcal{N}, \mathcal{L})$ specifies the grid topology and its three-phase incidence matrix $\mathbf{A}_{\mathfrak{B}}$ is given by:

$$\mathbf{A}_{\mathfrak{B}}: (\mathbf{A}_{\mathfrak{B}})_{kn} := \begin{cases} +\text{diag}(\mathbf{1}_3) & \text{if } \ell_k = (n, \cdot) \\ -\text{diag}(\mathbf{1}_3) & \text{if } \ell_k = (\cdot, n) \\ \mathbf{0}_{3 \times 3} & \text{otherwise} \end{cases}$$

- Vector of all nodal voltages and injected currents:

$$\begin{aligned} \mathbf{V}(f) &= \text{col}_{n \in \mathcal{N}}(\mathbf{v}_n(f)) \in \mathbb{C}^{3|\mathcal{N}| \times 1} \\ \mathbf{I}(f) &= \text{col}_{n \in \mathcal{N}}(\mathbf{i}_n(f)) \in \mathbb{C}^{3|\mathcal{N}| \times 1} \end{aligned}$$

- Similarly for the branch and shunt admittances:

$$\begin{aligned} \mathbf{Y}_{\mathcal{L}}(f) &= \text{diag}_{\ell \in \mathcal{L}}(\mathbf{y}_{\ell}(f)) \in \mathbb{C}^{3|\mathcal{L}| \times 3|\mathcal{L}|} \\ \mathbf{Y}_{\mathcal{T}}(f) &= \text{diag}_{t \in \mathcal{T}}(\mathbf{y}_t(f)) \in \mathbb{C}^{3|\mathcal{N}| \times 3|\mathcal{N}|} \end{aligned}$$

- Compound nodal admittance matrix:

$$\mathbf{I}(f) = \mathbf{Y}(f)\mathbf{V}(f), \mathbf{Y}(f) = \mathbf{A}_{\mathfrak{B}}^T \mathbf{Y}_{\mathcal{L}}(f) \mathbf{A}_{\mathfrak{B}} + \mathbf{Y}_{\mathcal{T}}(f)$$

- Nodal admittance equations w.r.t. \mathcal{S} and \mathcal{R} :

$$\begin{bmatrix} \mathbf{I}_{\mathcal{S}}(f) \\ \mathbf{I}_{\mathcal{R}}(f) \end{bmatrix} = \begin{bmatrix} \mathbf{Y}_{\mathcal{S} \times \mathcal{S}}(f) & \mathbf{Y}_{\mathcal{S} \times \mathcal{R}}(f) \\ \mathbf{Y}_{\mathcal{R} \times \mathcal{S}}(f) & \mathbf{Y}_{\mathcal{R} \times \mathcal{R}}(f) \end{bmatrix} \begin{bmatrix} \mathbf{V}_{\mathcal{S}}(f) \\ \mathbf{V}_{\mathcal{R}}(f) \end{bmatrix}$$

Grid Model – Hybrid Matrices (Single Frequency):

- Nodal admittance equations in block form w.r.t. \mathcal{S} and \mathcal{R} :

$$\begin{bmatrix} \mathbf{I}_{\mathcal{S}}(f) \\ \mathbf{I}_{\mathcal{R}}(f) \end{bmatrix} = \begin{bmatrix} \mathbf{Y}_{\mathcal{S} \times \mathcal{S}}(f) & \mathbf{Y}_{\mathcal{S} \times \mathcal{R}}(f) \\ \mathbf{Y}_{\mathcal{R} \times \mathcal{S}}(f) & \mathbf{Y}_{\mathcal{R} \times \mathcal{R}}(f) \end{bmatrix} \begin{bmatrix} \mathbf{V}_{\mathcal{S}}(f) \\ \mathbf{V}_{\mathcal{R}}(f) \end{bmatrix}$$

- Nodal hybrid equations:

$$\begin{bmatrix} \mathbf{V}_{\mathcal{S}}(f) \\ \mathbf{I}_{\mathcal{R}}(f) \end{bmatrix} = \begin{bmatrix} \mathbf{H}_{\mathcal{S} \times \mathcal{S}}(f) & \mathbf{H}_{\mathcal{S} \times \mathcal{R}}(f) \\ \mathbf{H}_{\mathcal{R} \times \mathcal{S}}(f) & \mathbf{H}_{\mathcal{R} \times \mathcal{R}}(f) \end{bmatrix} \begin{bmatrix} \mathbf{I}_{\mathcal{S}}(f) \\ \mathbf{V}_{\mathcal{R}}(f) \end{bmatrix}$$

- The individual blocks are given as (where $\mathbf{Y}/\mathbf{Y}_{\mathcal{R} \times \mathcal{R}}$ is the Schur complement of \mathbf{Y} w.r.t. $\mathbf{Y}_{\mathcal{R} \times \mathcal{R}}$):

$$\mathbf{H}_{\mathcal{S} \times \mathcal{S}}(f) = \mathbf{Y}_{\mathcal{S} \times \mathcal{S}}^{-1}(f)$$

$$\mathbf{H}_{\mathcal{S} \times \mathcal{R}}(f) = -\mathbf{Y}_{\mathcal{S} \times \mathcal{S}}^{-1}(f) \mathbf{Y}_{\mathcal{S} \times \mathcal{R}}(f)$$

$$\mathbf{H}_{\mathcal{R} \times \mathcal{S}}(f) = \mathbf{Y}_{\mathcal{R} \times \mathcal{S}}(f) \mathbf{Y}_{\mathcal{S} \times \mathcal{S}}^{-1}(f)$$

$$\mathbf{H}_{\mathcal{R} \times \mathcal{R}}(f) = \mathbf{Y}(f)/\mathbf{Y}_{\mathcal{R} \times \mathcal{R}}(f)$$

Grid Model – Hybrid Matrices (Harmonic-Domain Representation):

- Define the harmonic frequencies f_h w.r.t. the fundamental frequency f_1 as:
- Hybrid nodal equations can be written at each harmonic frequency.
- System of equations for the entire harmonic spectrum:

$$f_h := h \cdot f_1, \quad h \in \mathcal{H}$$

$$\begin{bmatrix} \hat{\mathbf{V}}_{\mathcal{S}} \\ \hat{\mathbf{I}}_{\mathcal{R}} \end{bmatrix} = \begin{bmatrix} \hat{\mathbf{H}}_{\mathcal{S} \times \mathcal{S}} & \hat{\mathbf{H}}_{\mathcal{S} \times \mathcal{R}} \\ \hat{\mathbf{H}}_{\mathcal{R} \times \mathcal{S}} & \hat{\mathbf{H}}_{\mathcal{R} \times \mathcal{R}} \end{bmatrix} \begin{bmatrix} \hat{\mathbf{I}}_{\mathcal{S}} \\ \hat{\mathbf{V}}_{\mathcal{R}} \end{bmatrix}$$

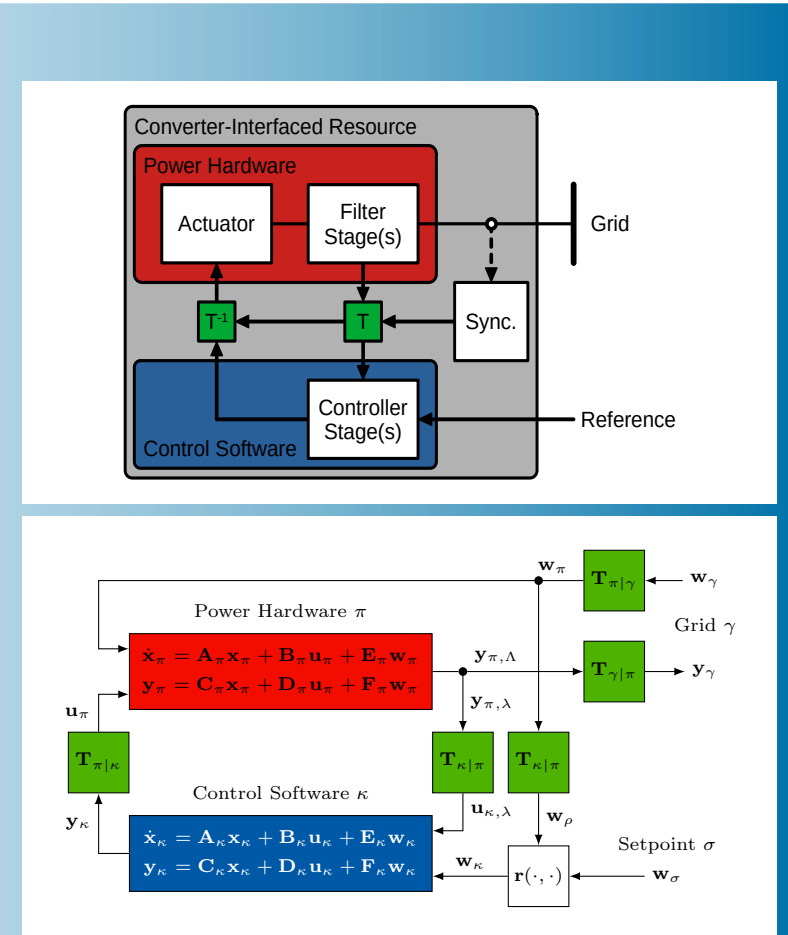
$$\hat{\mathbf{V}}_{\mathcal{S}} = \text{col}_{h \in \mathcal{H}}(\mathbf{v}_{\mathcal{S}}(f_h)) \in \mathbb{C}^{3|\mathcal{H}||\mathcal{S}| \times 1}$$

$$\hat{\mathbf{H}}_{\mathcal{S} \times \mathcal{S}} = \text{col}_{h \in \mathcal{H}}(\mathbf{H}_{\mathcal{S} \times \mathcal{S}}(f_h)) \in \mathbb{C}^{3|\mathcal{H}||\mathcal{S}| \times 3|\mathcal{H}||\mathcal{S}|}$$

⋮

Generic CIDER model:

- Classification based on its control law as grid-forming or –following CIDER.
- The CIDER is electrically connected to the grid, and obtains a reference from an upper-layer controller.
- Consists of:
 - Power hardware: Actuator (bridge), and a filter (L, LC, LCL or higher order).
 - Control software: controller stages (one or less per filter stage).
 - Transformations between (i) power hardware and grid and (ii) power hardware and control software.
 - Synchronization unit.
 - Reference calculation.
- All elements of the CIDER are represented by LTP functions or systems.



Examples for Transformations

External transform - $\tau_{\pi|\gamma}$ & $\tau_{\gamma|\pi}$:

- Four-wire CIDER (with neutral leg) connected to four-wire grid:
 - All sequences (positive, negative and homopolar) can flow.
- Three-wire CIDER connected to four-wire grid:
 - Homopolar sequences are blocked in both directions.

$$\mathbf{T}_{\pi|\gamma} = \mathbf{T}_{\gamma|\pi} = \text{diag}(\mathbf{1}_3)$$

$$\mathbf{T}_{\pi|\gamma} = \mathbf{T}_{\gamma|\pi} = \text{diag}(\mathbf{1}_3) - \frac{1}{3} \mathbf{1}_{3 \times 3}$$

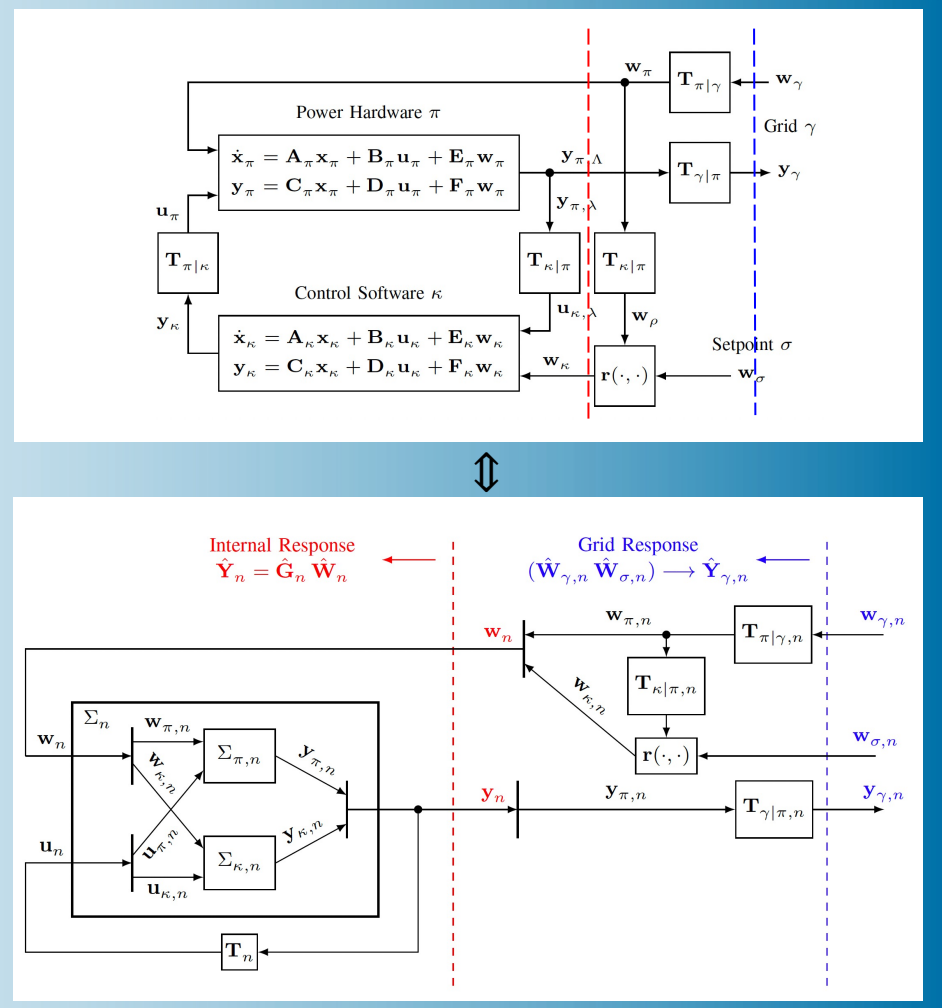
Internal transform - $\tau_{\pi|\kappa}$ & $\tau_{\kappa|\pi}$:

- Park (DQ) transformation:

$$\mathbf{T}_{\kappa|\pi} = \mathbf{T}_{\pi|\kappa}^T, \quad \mathbf{T}_{\pi|\kappa} = \sqrt{\frac{2}{3}} \begin{bmatrix} \cos(\theta(t)) & -\sin(\theta(t)) \\ \cos(\theta(t) - \frac{2\pi}{3}) & -\sin(\theta(t) - \frac{2\pi}{3}) \\ \cos(\theta(t) + \frac{2\pi}{3}) & -\sin(\theta(t) + \frac{2\pi}{3}) \end{bmatrix}$$

Generic CIDER Model (Derivation Overview):

- For the solution of the HPF one needs to derive the Grid Response of a CIDER n :
 - Formulation of the LTP models in time domain.
 - Transformation of those to harmonic domain using Toeplitz matrices.
 - Combination of power hardware and control software to form the open-loop system of the CIDER.
 - Derivation of the CIDER's internal response from the open-loop formulation and the internal transformations.
 - Representation of the reference calculation in harmonic domain.
 - Combination of internal response, reference calculation and external transformations to form the grid response.
 - Derivation of the partial derivatives needed for the Newton-Raphson solution.
- Furthermore, it is shown how to approximate nonlinearities within the internal response for the generic model of the CIDER.



Generic CIDER Model (Time Domain):

- In- and output quantities:

- Grid-forming CIDER:
 - Grid-following CIDER

$$\mathbf{w}_\gamma(t) \sim \mathbf{i}(t), \quad \mathbf{y}_\gamma(t) \sim \mathbf{v}(t), \quad \mathbf{w}_\sigma(t) \sim V, f$$

- Power hardware π :

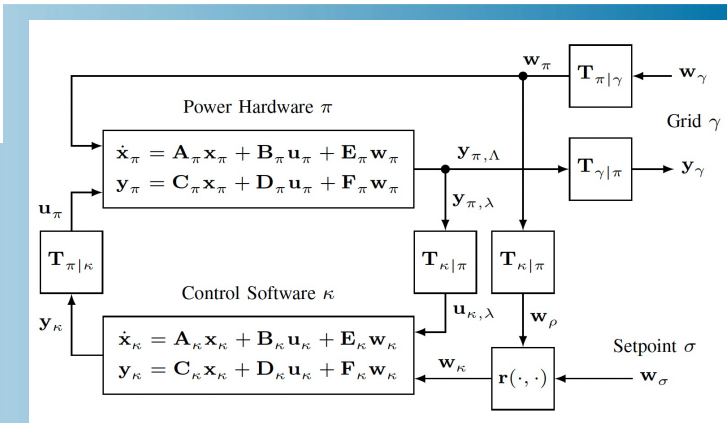
- Control software κ :

- Transformations:

- From π to κ and vice versa $\tau_{\pi|\kappa}$ & $\tau_{\kappa|\pi}$:
 - From π to grid γ and vice versa $\tau_{\pi|\gamma}$ & $\tau_{\gamma|\pi}$:

- Reference calculation ρ :

Transformed to harmonic domain using Fourier and Toeplitz theory.



$$\begin{aligned}\dot{\mathbf{x}}_\pi(t) &= \mathbf{A}_\pi(t)\mathbf{x}_\pi(t) + \mathbf{B}_\pi(t)\mathbf{u}_\pi(t) + \mathbf{E}_\pi(t)\mathbf{w}_\pi(t) \\ \mathbf{y}_\pi(t) &= \mathbf{C}_\pi(t)\mathbf{x}_\pi(t) + \mathbf{D}_\pi(t)\mathbf{u}_\pi(t) + \mathbf{F}_\pi(t)\mathbf{w}_\pi(t)\end{aligned}$$

$$\begin{aligned}\dot{\mathbf{x}}_\kappa(t) &= \mathbf{A}_\kappa(t)\mathbf{x}_\kappa(t) + \mathbf{B}_\kappa(t)\mathbf{u}_\kappa(t) + \mathbf{E}_\kappa(t)\mathbf{w}_\kappa(t) \\ \mathbf{y}_\kappa(t) &= \mathbf{C}_\kappa(t)\mathbf{x}_\kappa(t) + \mathbf{D}_\kappa(t)\mathbf{u}_\kappa(t) + \mathbf{F}_\kappa(t)\mathbf{w}_\kappa(t)\end{aligned}$$

$$\mathbf{u}_\pi(t) = \mathbf{T}_{\pi|\kappa}(t)\mathbf{y}_\kappa(t), \quad \mathbf{u}_\kappa(t) = \mathbf{T}_{\kappa|\pi}^+(t)\mathbf{y}_\pi(t)$$

$$\mathbf{w}_\kappa(t) = \mathbf{r}(\mathbf{w}_\rho(t), \mathbf{w}_\sigma(t))$$

Generic CIDER Model (Harmonic Domain):

- Power hardware,
with $\widehat{\Omega}_\pi = 2\pi f_1 \text{diag}_{h \in \mathcal{H}}(h \cdot \mathbf{1}_\pi)$:

$$j\widehat{\Omega}_\pi \widehat{\mathbf{X}}_\pi = \widehat{\mathbf{A}}_\pi \widehat{\mathbf{X}}_\pi + \widehat{\mathbf{B}}_\pi \widehat{\mathbf{U}}_\pi + \widehat{\mathbf{E}}_\pi \widehat{\mathbf{W}}_\pi$$

$$\widehat{\mathbf{Y}}_\pi = \widehat{\mathbf{C}}_\pi \widehat{\mathbf{X}}_\pi + \widehat{\mathbf{D}}_\pi \widehat{\mathbf{U}}_\pi + \widehat{\mathbf{F}}_\pi \widehat{\mathbf{W}}_\pi$$

$$j\widehat{\Omega}_\kappa \widehat{\mathbf{X}}_\kappa = \widehat{\mathbf{A}}_\kappa \widehat{\mathbf{X}}_\kappa + \widehat{\mathbf{B}}_\kappa \widehat{\mathbf{U}}_\kappa + \widehat{\mathbf{E}}_\kappa \widehat{\mathbf{W}}_\kappa$$

$$\widehat{\mathbf{Y}}_\kappa = \widehat{\mathbf{C}}_\kappa \widehat{\mathbf{X}}_\kappa + \widehat{\mathbf{D}}_\kappa \widehat{\mathbf{U}}_\kappa + \widehat{\mathbf{F}}_\kappa \widehat{\mathbf{W}}_\kappa$$

- Transformations:

$$\widehat{\mathbf{U}}_\kappa = \widehat{\mathbf{T}}_{\kappa|\pi}^+ \widehat{\mathbf{Y}}_\pi$$

$$\widehat{\mathbf{U}}_\pi = \widehat{\mathbf{T}}_{\pi|\kappa} \widehat{\mathbf{Y}}_\kappa$$

- Closed-loop system of the CIDER:

- Closed-loop transfer function:

Generic CIDER Model (Harmonic Domain):

- Power hardware,
with $\widehat{\Omega}_\pi = 2\pi f_1 \text{diag}_{h \in \mathcal{H}}(h \cdot \mathbf{1}_\pi)$:

- Control software,
with $\widehat{\Omega}_\kappa = 2\pi f_1 \text{diag}_{h \in \mathcal{H}}(h \cdot \mathbf{1}_\kappa)$:

- Transformations:

- Closed-loop system of the CIDER:

- Closed-loop transfer function:

$$\begin{aligned} j\widehat{\Omega}_\pi \widehat{\mathbf{X}}_\pi &= \widehat{\mathbf{A}}_\pi \widehat{\mathbf{X}}_\pi + \widehat{\mathbf{B}}_\pi \widehat{\mathbf{U}}_\pi + \widehat{\mathbf{E}}_\pi \widehat{\mathbf{W}}_\pi \\ \widehat{\mathbf{Y}}_\pi &= \widehat{\mathbf{C}}_\pi \widehat{\mathbf{X}}_\pi + \widehat{\mathbf{D}}_\pi \widehat{\mathbf{U}}_\pi + \widehat{\mathbf{F}}_\pi \widehat{\mathbf{W}}_\pi \end{aligned}$$

$$\begin{aligned} j\widehat{\Omega}_\kappa \widehat{\mathbf{X}}_\kappa &= \widehat{\mathbf{A}}_\kappa \widehat{\mathbf{X}}_\kappa + \widehat{\mathbf{B}}_\kappa \widehat{\mathbf{U}}_\kappa + \widehat{\mathbf{E}}_\kappa \widehat{\mathbf{W}}_\kappa \\ \widehat{\mathbf{Y}}_\kappa &= \widehat{\mathbf{C}}_\kappa \widehat{\mathbf{X}}_\kappa + \widehat{\mathbf{D}}_\kappa \widehat{\mathbf{U}}_\kappa + \widehat{\mathbf{F}}_\kappa \widehat{\mathbf{W}}_\kappa \end{aligned}$$

$$\begin{aligned} \widehat{\mathbf{U}}_\kappa &= \widehat{\mathbf{T}}_{\kappa|\pi}^+ \widehat{\mathbf{Y}}_\pi \\ \widehat{\mathbf{U}}_\pi &= \widehat{\mathbf{T}}_{\pi|\kappa} \widehat{\mathbf{Y}}_\kappa \end{aligned}$$

Open-loop system of the CIDER:

$$j\widehat{\Omega} \widehat{\mathbf{X}} = \widehat{\mathbf{A}} \widehat{\mathbf{X}} + \widehat{\mathbf{B}} \widehat{\mathbf{U}} + \widehat{\mathbf{E}} \widehat{\mathbf{W}}$$

$$\widehat{\mathbf{Y}} = \widehat{\mathbf{C}} \widehat{\mathbf{X}} + \widehat{\mathbf{D}} \widehat{\mathbf{U}} + \widehat{\mathbf{F}} \widehat{\mathbf{W}}$$

$$\widehat{\mathbf{X}} = \text{col}(\widehat{\mathbf{X}}_\pi, \widehat{\mathbf{X}}_\kappa), \dots \text{ & } \widehat{\mathbf{A}} = \text{col}(\widehat{\mathbf{A}}_\pi, \widehat{\mathbf{A}}_\kappa), \dots$$

$$\widehat{\mathbf{U}} = \widehat{\mathbf{T}} \widehat{\mathbf{Y}}, \widehat{\mathbf{T}} = \begin{bmatrix} \mathbf{0} & \widehat{\mathbf{T}}_{\pi|\kappa} \\ \widehat{\mathbf{T}}_{\kappa|\pi}^+ & \mathbf{0} \end{bmatrix}$$

Generic CIDER Model (Harmonic Domain):

- Power hardware,
with $\widehat{\Omega}_\pi = 2\pi f_1 \text{diag}_{h \in \mathcal{H}}(h \cdot \mathbf{1}_\pi)$:

- Control software,
with $\widehat{\Omega}_\kappa = 2\pi f_1 \text{diag}_{h \in \mathcal{H}}(h \cdot \mathbf{1}_\kappa)$:

- Transformations:

- Closed-loop system of the CIDER:

- Closed-loop transfer function:

$$\begin{aligned} j\widehat{\Omega}_\pi \widehat{\mathbf{X}}_\pi &= \widehat{\mathbf{A}}_\pi \widehat{\mathbf{X}}_\pi + \widehat{\mathbf{B}}_\pi \widehat{\mathbf{U}}_\pi + \widehat{\mathbf{E}}_\pi \widehat{\mathbf{W}}_\pi \\ \widehat{\mathbf{Y}}_\pi &= \widehat{\mathbf{C}}_\pi \widehat{\mathbf{X}}_\pi + \widehat{\mathbf{D}}_\pi \widehat{\mathbf{U}}_\pi + \widehat{\mathbf{F}}_\pi \widehat{\mathbf{W}}_\pi \end{aligned}$$

$$\begin{aligned} j\widehat{\Omega}_\kappa \widehat{\mathbf{X}}_\kappa &= \widehat{\mathbf{A}}_\kappa \widehat{\mathbf{X}}_\kappa + \widehat{\mathbf{B}}_\kappa \widehat{\mathbf{U}}_\kappa + \widehat{\mathbf{E}}_\kappa \widehat{\mathbf{W}}_\kappa \\ \widehat{\mathbf{Y}}_\kappa &= \widehat{\mathbf{C}}_\kappa \widehat{\mathbf{X}}_\kappa + \widehat{\mathbf{D}}_\kappa \widehat{\mathbf{U}}_\kappa + \widehat{\mathbf{F}}_\kappa \widehat{\mathbf{W}}_\kappa \end{aligned}$$

$$\begin{aligned} \widehat{\mathbf{U}}_\kappa &= \widehat{\mathbf{T}}_{\kappa|\pi}^+ \widehat{\mathbf{Y}}_\pi \\ \widehat{\mathbf{U}}_\pi &= \widehat{\mathbf{T}}_{\pi|\kappa} \widehat{\mathbf{Y}}_\kappa \end{aligned}$$

$$\begin{aligned} j\widehat{\Omega} \widehat{\mathbf{X}} &= \widetilde{\mathbf{A}} \widehat{\mathbf{X}} + \widetilde{\mathbf{E}} \widehat{\mathbf{W}} \\ \widehat{\mathbf{Y}} &= \widetilde{\mathbf{C}} \widehat{\mathbf{X}} + \widetilde{\mathbf{F}} \widehat{\mathbf{W}} \end{aligned}$$

Open-loop system of the CIDER:

$$j\widehat{\Omega} \widehat{\mathbf{X}} = \widehat{\mathbf{A}} \widehat{\mathbf{X}} + \widehat{\mathbf{B}} \widehat{\mathbf{U}} + \widehat{\mathbf{E}} \widehat{\mathbf{W}}$$

$$\widehat{\mathbf{Y}} = \widehat{\mathbf{C}} \widehat{\mathbf{X}} + \widehat{\mathbf{D}} \widehat{\mathbf{U}} + \widehat{\mathbf{F}} \widehat{\mathbf{W}}$$

$$\widehat{\mathbf{X}} = \text{col}(\widehat{\mathbf{X}}_\pi, \widehat{\mathbf{X}}_\kappa), \dots \text{ & } \widehat{\mathbf{A}} = \text{col}(\widehat{\mathbf{A}}_\pi, \widehat{\mathbf{A}}_\kappa), \dots$$

$$\widehat{\mathbf{U}} = \widehat{\mathbf{T}} \widehat{\mathbf{Y}}, \widehat{\mathbf{T}} = \begin{bmatrix} \mathbf{0} & \widehat{\mathbf{T}}_{\pi|\kappa} \\ \widehat{\mathbf{T}}_{\kappa|\pi}^+ & \mathbf{0} \end{bmatrix}$$

$$\begin{aligned} \widetilde{\mathbf{A}} &= \widehat{\mathbf{A}} + \widehat{\mathbf{B}} (\text{diag}(\mathbf{1}) - \widehat{\mathbf{T}} \widehat{\mathbf{D}})^{-1} \widehat{\mathbf{T}} \widehat{\mathbf{C}} \\ \widetilde{\mathbf{E}} &= \widehat{\mathbf{E}} + \widehat{\mathbf{B}} (\text{diag}(\mathbf{1}) - \widehat{\mathbf{T}} \widehat{\mathbf{D}})^{-1} \widehat{\mathbf{T}} \widehat{\mathbf{F}} \\ \widetilde{\mathbf{C}} &= (\text{diag}(\mathbf{1}) - \widehat{\mathbf{D}} \widehat{\mathbf{T}})^{-1} \widehat{\mathbf{C}} \\ \widetilde{\mathbf{F}} &= (\text{diag}(\mathbf{1}) - \widehat{\mathbf{D}} \widehat{\mathbf{T}})^{-1} \widehat{\mathbf{F}} \end{aligned}$$

$$\widehat{\mathbf{Y}} = \widehat{\mathbf{G}} \widehat{\mathbf{W}}, \widehat{\mathbf{G}} = \widetilde{\mathbf{C}} (j\widehat{\Omega} - \widetilde{\mathbf{A}})^{-1} \widetilde{\mathbf{E}} + \widetilde{\mathbf{F}}$$

Generic CIDER Model (Harmonic Domain):

- Reference Calculation:

- $\widehat{\mathbf{R}}(\cdot, \cdot)$ approximates $\mathbf{r}(\cdot, \cdot)$.
- $\widehat{\mathbf{R}}(\cdot, \cdot)$ is differentiable.

Needed for the numerical solution of the HPF.

- Closed-loop transfer function in block form:

$$\widehat{\mathbf{W}}_\kappa \approx \widehat{\mathbf{R}}(\widehat{\mathbf{W}}_\rho, \widehat{\mathbf{W}}_\sigma) = \widehat{\mathbf{R}}(\widehat{\mathbf{W}}_\sigma, \widehat{\mathbf{T}}_{\kappa|\pi} \widehat{\mathbf{W}}_\pi)$$

- Internal response $\widehat{\mathbf{Y}}_\pi$:

$$\begin{bmatrix} \widehat{\mathbf{Y}}_\pi \\ \widehat{\mathbf{Y}}_\kappa \end{bmatrix} = \begin{bmatrix} \widehat{\mathbf{G}}_{\pi\pi} & \widehat{\mathbf{G}}_{\pi\kappa} \\ \widehat{\mathbf{G}}_{\kappa\pi} & \widehat{\mathbf{G}}_{\kappa\kappa} \end{bmatrix} \begin{bmatrix} \widehat{\mathbf{W}}_\pi \\ \widehat{\mathbf{W}}_\kappa \end{bmatrix}$$

- Grid response $\widehat{\mathbf{Y}}_\gamma$:

$$\widehat{\mathbf{Y}}_\pi = \widehat{\mathbf{G}}_{\pi\pi} \widehat{\mathbf{W}}_\pi + \widehat{\mathbf{G}}_{\pi\kappa} \widehat{\mathbf{W}}_\kappa$$

$$\Leftrightarrow \widehat{\mathbf{Y}}_\pi(\widehat{\mathbf{W}}_\pi, \widehat{\mathbf{W}}_\sigma) = \widehat{\mathbf{G}}_{\pi\pi} \widehat{\mathbf{W}}_\pi + \widehat{\mathbf{G}}_{\pi\kappa} \widehat{\mathbf{R}}(\widehat{\mathbf{W}}_\sigma, \widehat{\mathbf{T}}_{\kappa|\pi} \widehat{\mathbf{W}}_\pi)$$

- Partial derivative of $\widehat{\mathbf{Y}}_\gamma$ w.r.t. $\widehat{\mathbf{W}}_\gamma$:

- Obtained using the chain rule.
- $\partial_\gamma, \partial_\pi, \partial_\rho$: partial derivatives w.r.t. $\widehat{\mathbf{W}}_\gamma, \widehat{\mathbf{W}}_\pi, \widehat{\mathbf{W}}_\rho$.

$$\widehat{\mathbf{Y}}_\gamma = \widehat{\mathbf{T}}_{\gamma|\pi}^+ \widehat{\mathbf{Y}}_\pi = \widehat{\mathbf{T}}_{\gamma|\pi}^+ \cdot \widehat{\mathbf{Y}}_\pi(\widehat{\mathbf{W}}_\pi, \widehat{\mathbf{W}}_\sigma)$$

$$\Leftrightarrow \widehat{\mathbf{Y}}_\gamma(\widehat{\mathbf{W}}_\gamma, \widehat{\mathbf{W}}_\sigma) = \widehat{\mathbf{T}}_{\gamma|\pi}^+ \cdot \widehat{\mathbf{Y}}_\pi(\widehat{\mathbf{T}}_{\pi|\gamma} \widehat{\mathbf{W}}_\gamma, \widehat{\mathbf{W}}_\sigma)$$

$$\partial_\gamma \widehat{\mathbf{Y}}_\gamma(\widehat{\mathbf{W}}_\gamma, \widehat{\mathbf{W}}_\sigma) = \widehat{\mathbf{T}}_{\gamma|\pi}^+ \cdot \partial_\pi \widehat{\mathbf{Y}}_\pi(\widehat{\mathbf{T}}_{\pi|\gamma} \widehat{\mathbf{W}}_\gamma, \widehat{\mathbf{W}}_\sigma) \widehat{\mathbf{T}}_{\pi|\gamma}$$

$$\partial_\pi \widehat{\mathbf{Y}}_\pi(\widehat{\mathbf{W}}_\pi, \widehat{\mathbf{W}}_\sigma) = \widehat{\mathbf{G}}_{\pi\pi} + \widehat{\mathbf{G}}_{\pi\kappa} \partial_\rho \widehat{\mathbf{R}}(\widehat{\mathbf{W}}_\sigma, \widehat{\mathbf{T}}_{\kappa|\pi} \widehat{\mathbf{W}}_\pi) \widehat{\mathbf{T}}_{\kappa|\pi}$$

Generic CIDER Model (Harmonic Domain):

- Open-loop model of a CIDER n in time domain:

$$\dot{\mathbf{x}}_n(t) = \mathbf{A}_n(t)\mathbf{x}_n(t) + \mathbf{B}_n(t)\mathbf{u}_n(t) + \mathbf{E}_n(t)\mathbf{w}_n(t)$$

$$\mathbf{y}_n(t) = \mathbf{C}_n(t)\mathbf{x}_n(t) + \mathbf{D}_n(t)\mathbf{u}_n(t) + \mathbf{F}_n(t)\mathbf{w}_n(t)$$

- Nonlinearities within the internal response of the CIDER:

- Locally approximate the internal response through linearization w.r.t. an operating point $\mathbf{y}_{o,n}(t)$.

➤ Matrices become a function of the operating point:

➤ Resulting internal response:

➤ Resulting grid response:

Operating point does not need to be constant, but can consist of time-periodic trajectories.

$$\mathbf{A}_n: \mathbf{A}_n(t, \mathbf{y}_{o,n}(t)), \mathbf{B}_n: \dots$$

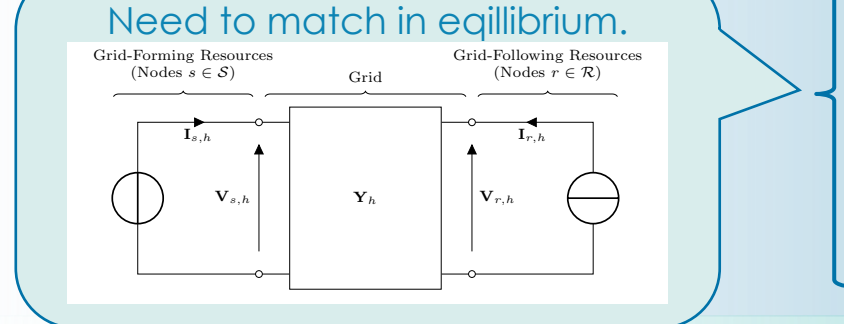
$$\widehat{\mathbf{Y}}_n(\widehat{\mathbf{W}}_n, \widehat{\mathbf{Y}}_{o,n}) = \widehat{\mathbf{G}}_n(\widehat{\mathbf{Y}}_{o,n})\widehat{\mathbf{W}}_n$$

$$\begin{aligned} \widehat{\mathbf{Y}}_{\gamma,n}(\widehat{\mathbf{W}}_{\gamma,n}, \widehat{\mathbf{W}}_{\sigma,n}, \widehat{\mathbf{Y}}_{o,n}) \\ = \widehat{\mathbf{T}}_{\gamma|\pi,n}^+ \cdot \widehat{\mathbf{Y}}_{\pi,n}(\widehat{\mathbf{T}}_{\pi|\gamma,n}\widehat{\mathbf{W}}_{\gamma,n}, \widehat{\mathbf{W}}_{\sigma,n}, \widehat{\mathbf{Y}}_{o,n}) \end{aligned}$$

Mismatch Equations and Their Partial Derivatives:

- Nodal equations from point of view of the:

- Grid:



- Resources:

- Mismatch equations of the entire system:

➤ Solved using the Newton-Raphson method.

➤ Partial derivatives for the Jacobian matrix:

- Grid:

- Resources:

$$\hat{\mathbf{V}}_S(\hat{\mathbf{I}}_S, \hat{\mathbf{V}}_R) = \hat{\mathbf{H}}_{S \times S} \hat{\mathbf{I}}_S + \hat{\mathbf{H}}_{S \times R} \hat{\mathbf{V}}_R$$

$$\hat{\mathbf{I}}_R(\hat{\mathbf{I}}_S, \hat{\mathbf{V}}_R) = \hat{\mathbf{H}}_{R \times S} \hat{\mathbf{I}}_S + \hat{\mathbf{H}}_{R \times R} \hat{\mathbf{V}}_R$$

$$s \in \mathcal{S}: \hat{\mathbf{V}}_S(\hat{\mathbf{I}}_S, V_{\sigma,s}, f_{\sigma,s}) = \hat{\mathbf{Y}}_{\gamma,S}(\hat{\mathbf{T}}_{\pi|\gamma} \hat{\mathbf{I}}_S, V_{\sigma,s}, f_{\sigma,s})$$

$$r \in \mathcal{R}: \hat{\mathbf{I}}_R(\hat{\mathbf{V}}_R, S_{\sigma,r}) = \hat{\mathbf{Y}}_{\gamma,R}(\hat{\mathbf{T}}_{\pi|\gamma} \hat{\mathbf{V}}_R, S_{\sigma,r})$$

$$\Delta \hat{\mathbf{V}}_S(\hat{\mathbf{I}}_S, \hat{\mathbf{V}}_R, V_\sigma, f_\sigma) = \mathbf{0}$$

$$\Delta \hat{\mathbf{I}}_R(\hat{\mathbf{I}}_S, \hat{\mathbf{V}}_R, S_\sigma) = \mathbf{0}$$

$$\partial_S \hat{\mathbf{V}}_S(\hat{\mathbf{I}}_S, \hat{\mathbf{V}}_R) = \hat{\mathbf{H}}_{S \times S}, \partial_R \hat{\mathbf{V}}_S(\hat{\mathbf{I}}_S, \hat{\mathbf{V}}_R) = \hat{\mathbf{H}}_{S \times R}$$

$$\partial_S \hat{\mathbf{I}}_R(\hat{\mathbf{I}}_S, \hat{\mathbf{V}}_R) = \hat{\mathbf{H}}_{R \times S}, \partial_R \hat{\mathbf{I}}_R(\hat{\mathbf{I}}_S, \hat{\mathbf{V}}_R) = \hat{\mathbf{H}}_{R \times R}$$

$$s \in \mathcal{S}: \partial_S \hat{\mathbf{V}}_S(\hat{\mathbf{I}}_S, V_{\sigma,s}, f_{\sigma,s}) = \partial_\gamma \hat{\mathbf{Y}}_\gamma(\hat{\mathbf{T}}_{\pi|\gamma} \hat{\mathbf{I}}_S, V_{\sigma,s}, f_{\sigma,s})$$

$$r \in \mathcal{R}: \partial_r \hat{\mathbf{I}}_R(\hat{\mathbf{V}}_R, S_{\sigma,r}) = \partial_\gamma \hat{\mathbf{Y}}_{\gamma,R}(\hat{\mathbf{T}}_{\pi|\gamma} \hat{\mathbf{V}}_R, S_{\sigma,r})$$

Newton-Raphson Solution of the HPF Problem

- The algorithm is single-iterative, thanks to inclusion of the CIDER closed-loop transfer functions into the mismatch equations.
- Lines 3-4: Initialization.
 - Injected currents of nodes with grid-forming resources are set to 0.
 - Nodal voltages of nodes with grid-following resources are set to a pure positive sequence with magnitude 1 p.u. in the fundamental.
- Lines 7-8: Computation of the residuals from the nodal equations of the grid and the resources.
- Lines 10-13: Computation of the Jacobian matrix from the partial derivatives.
- Line 15: Newton-Raphson iteration.
- Line 16: Update of the nodal quantities.

Algorithm 1 Newton-Raphson solution of the HPF problem.

```

1: procedure HPF( $\Delta\hat{\mathbf{V}}_S(\cdot, \cdot, \cdot)$ ,  $\Delta\hat{\mathbf{I}}_R(\cdot, \cdot, \cdot)$ ,  $\mathbf{V}_\sigma$ ,  $\mathbf{f}_\sigma$ ,  $\mathbf{S}_\sigma$ )
2:   # Initialization
3:    $\hat{\mathbf{I}}_S \leftarrow \mathbf{0}$ 
4:    $\hat{\mathbf{V}}_R \leftarrow \text{flat\_start}()$ 
5:   while  $\max(|\Delta\hat{\mathbf{V}}_S|, |\Delta\hat{\mathbf{I}}_R|) \geq \epsilon$  do
6:     # Residuals
7:      $\Delta\hat{\mathbf{V}}_S \leftarrow \Delta\hat{\mathbf{V}}_S(\hat{\mathbf{I}}_S, \hat{\mathbf{V}}_R, \mathbf{V}_\sigma, \mathbf{f}_\sigma)$ 
8:      $\Delta\hat{\mathbf{I}}_R \leftarrow \Delta\hat{\mathbf{I}}_R(\hat{\mathbf{I}}_S, \hat{\mathbf{V}}_R, \mathbf{S}_\sigma)$ 
9:     # Jacobian matrix
10:     $\hat{\mathbf{J}}_{S \times S} \leftarrow \partial_S \Delta\hat{\mathbf{V}}_S(\hat{\mathbf{I}}_S, \hat{\mathbf{V}}_R, \mathbf{V}_\sigma, \mathbf{f}_\sigma)$ 
11:     $\hat{\mathbf{J}}_{S \times R} \leftarrow \partial_R \Delta\hat{\mathbf{V}}_S(\hat{\mathbf{I}}_S, \hat{\mathbf{V}}_R, \mathbf{V}_\sigma, \mathbf{f}_\sigma)$ 
12:     $\hat{\mathbf{J}}_{R \times S} \leftarrow \partial_S \Delta\hat{\mathbf{I}}_R(\hat{\mathbf{I}}_S, \hat{\mathbf{V}}_R, \mathbf{S}_\sigma)$ 
13:     $\hat{\mathbf{J}}_{R \times R} \leftarrow \partial_R \Delta\hat{\mathbf{I}}_R(\hat{\mathbf{I}}_S, \hat{\mathbf{V}}_R, \mathbf{S}_\sigma)$ 
14:    # Newton-Raphson iteration
15:    
$$\begin{bmatrix} \Delta\hat{\mathbf{I}}_S \\ \Delta\hat{\mathbf{V}}_R \end{bmatrix} \leftarrow \begin{bmatrix} \hat{\mathbf{J}}_{S \times S} & \hat{\mathbf{J}}_{S \times R} \\ \hat{\mathbf{J}}_{R \times S} & \hat{\mathbf{J}}_{R \times R} \end{bmatrix}^{-1} \begin{bmatrix} \Delta\hat{\mathbf{V}}_S \\ \Delta\hat{\mathbf{I}}_R \end{bmatrix}$$

16:    
$$\begin{bmatrix} \hat{\mathbf{I}}_S \\ \hat{\mathbf{V}}_R \end{bmatrix} \leftarrow \begin{bmatrix} \hat{\mathbf{I}}_S \\ \hat{\mathbf{V}}_R \end{bmatrix} - \begin{bmatrix} \Delta\hat{\mathbf{I}}_S \\ \Delta\hat{\mathbf{V}}_R \end{bmatrix}$$

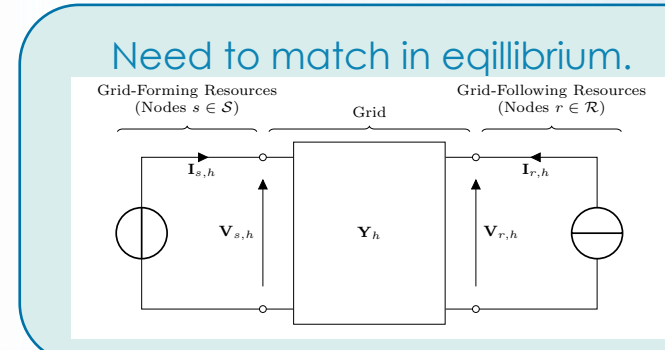
17:  end while
18: end procedure

```

Mismatch Equations and Their Partial Derivatives Including Linearizations:

- Nodal equations from point of view of the :

- Grid:



- Resources:

- Mismatch equations of the entire system:

➤ Solved using the Newton Raphson method.

➤ Partial derivatives for the Jacobian matrix:

- Grid:

- Resources:

$$\hat{\mathbf{V}}_S(\hat{\mathbf{I}}_S, \hat{\mathbf{V}}_R) = \hat{\mathbf{H}}_{S \times S} \hat{\mathbf{I}}_S + \hat{\mathbf{H}}_{S \times R} \hat{\mathbf{V}}_R$$

$$\hat{\mathbf{I}}_R(\hat{\mathbf{I}}_S, \hat{\mathbf{V}}_R) = \hat{\mathbf{H}}_{R \times S} \hat{\mathbf{I}}_S + \hat{\mathbf{H}}_{R \times R} \hat{\mathbf{V}}_R$$

$$s \in \mathcal{S}: \hat{\mathbf{V}}_S(\hat{\mathbf{I}}_S, V_{\sigma,S}, f_{\sigma,S}, \hat{\mathbf{Y}}_{o,S}) = \hat{\mathbf{Y}}_{\gamma,S}(\hat{\mathbf{T}}_{\pi|\gamma} \hat{\mathbf{I}}_S, V_{\sigma,S}, f_{\sigma,S}, \hat{\mathbf{Y}}_{o,S})$$

$$r \in \mathcal{R}: \hat{\mathbf{I}}_R(\hat{\mathbf{V}}_R, S_{\sigma,r}, \hat{\mathbf{Y}}_{o,r}) = \hat{\mathbf{Y}}_{\gamma,r}(\hat{\mathbf{T}}_{\pi|\gamma} \hat{\mathbf{V}}_R, S_{\sigma,r}, \hat{\mathbf{Y}}_{o,r})$$

$$\Delta \hat{\mathbf{V}}_S(\hat{\mathbf{I}}_S, \hat{\mathbf{V}}_R, V_{\sigma}, f_{\sigma}, \hat{\mathbf{Y}}_{o,S}) = \mathbf{0}$$

$$\Delta \hat{\mathbf{I}}_R(\hat{\mathbf{I}}_S, \hat{\mathbf{V}}_R, S_{\sigma}, \hat{\mathbf{Y}}_{o,R}) = \mathbf{0}$$

$$\partial_S \hat{\mathbf{V}}_S(\hat{\mathbf{I}}_S, \hat{\mathbf{V}}_R) = \hat{\mathbf{H}}_{S \times S}, \partial_R \hat{\mathbf{V}}_S(\hat{\mathbf{I}}_S, \hat{\mathbf{V}}_R) = \hat{\mathbf{H}}_{S \times R}$$

$$\partial_S \hat{\mathbf{I}}_R(\hat{\mathbf{I}}_S, \hat{\mathbf{V}}_R) = \hat{\mathbf{H}}_{R \times S}, \partial_R \hat{\mathbf{I}}_R(\hat{\mathbf{I}}_S, \hat{\mathbf{V}}_R) = \hat{\mathbf{H}}_{R \times R}$$

$$s \in \mathcal{S}: \partial_S \hat{\mathbf{V}}_S(\hat{\mathbf{I}}_S, V_{\sigma,S}, f_{\sigma,S}, \hat{\mathbf{Y}}_{o,S}) = \partial_\gamma \hat{\mathbf{Y}}_\gamma(\hat{\mathbf{T}}_{\pi|\gamma} \hat{\mathbf{I}}_S, V_{\sigma,S}, f_{\sigma,S}, \hat{\mathbf{Y}}_{o,S})$$

$$r \in \mathcal{R}: \partial_r \hat{\mathbf{I}}_R(\hat{\mathbf{V}}_R, S_{\sigma,r}, \hat{\mathbf{Y}}_{o,r}) = \partial_\gamma \hat{\mathbf{Y}}_{\gamma,r}(\hat{\mathbf{T}}_{\pi|\gamma} \hat{\mathbf{V}}_R, S_{\sigma,r}, \hat{\mathbf{Y}}_{o,r})$$

Newton-Raphson Solution of the HPF Problem Including Linearizations

- The algorithm is single-iterative, thanks to inclusion of the CIDER closed-loop transfer functions into the mismatch equations.
- Lines 3-6: Initialization.
 - Injected currents of nodes with grid-forming resources are set to 0.
 - Nodal voltages of nodes with grid-following resources are set to a pure positive sequence with magnitude 1p.u. in the fundamental.
 - Operating points are set to nominal or reference values.
- Lines 9-10: Computation of the residuals from the nodal equations of the grid and the resources, taking into account the operating point.
- Lines 12-15: Computation of the Jacobian matrix from the partial derivatives , taking into account the operating point.
- Line 17: Newton-Raphson iteration.
- Line 18: Update of the nodal quantities.
- Lines 20-21: Update of the operating points from the CIDER's internal responses.

Algorithm 2 Newton-Raphson solution of the HPF problem.

```

1: procedure HPF( $\Delta\hat{\mathbf{V}}_S(\cdot, \cdot, \cdot)$ ,  $\Delta\hat{\mathbf{I}}_R(\cdot, \cdot, \cdot)$ ,  $\mathbf{V}_\sigma$ ,  $\mathbf{f}_\sigma$ ,  $\mathbf{S}_\sigma$ )
2:   # Initialization
3:    $\hat{\mathbf{I}}_S \leftarrow \mathbf{0}$ 
4:    $\hat{\mathbf{V}}_R \leftarrow \text{flat\_start}()$ 
5:    $\hat{\mathbf{Y}}_{o,S} \leftarrow \text{initialize\_operating\_point}()$ 
6:    $\hat{\mathbf{Y}}_{o,R} \leftarrow \text{initialize\_operating\_point}()$ 
7:   while  $\max(|\Delta\hat{\mathbf{V}}_S|, |\Delta\hat{\mathbf{I}}_R|) \geq \epsilon$  do
8:     # Residuals
9:      $\Delta\hat{\mathbf{V}}_S \leftarrow \Delta\hat{\mathbf{V}}_S(\hat{\mathbf{I}}_S, \hat{\mathbf{V}}_R, \mathbf{V}_\sigma, \mathbf{f}_\sigma, \hat{\mathbf{Y}}_{o,S})$ 
10:     $\Delta\hat{\mathbf{I}}_R \leftarrow \Delta\hat{\mathbf{I}}_R(\hat{\mathbf{I}}_S, \hat{\mathbf{V}}_R, \mathbf{S}_\sigma, \hat{\mathbf{Y}}_{o,R})$ 
11:    # Jacobian matrix
12:     $\hat{\mathbf{J}}_{S \times S} \leftarrow \partial_S \Delta\hat{\mathbf{V}}_S(\hat{\mathbf{I}}_S, \hat{\mathbf{V}}_R, \mathbf{V}_\sigma, \mathbf{f}_\sigma, \hat{\mathbf{Y}}_{o,S})$ 
13:     $\hat{\mathbf{J}}_{S \times R} \leftarrow \partial_R \Delta\hat{\mathbf{V}}_S(\hat{\mathbf{I}}_S, \hat{\mathbf{V}}_R, \mathbf{V}_\sigma, \mathbf{f}_\sigma, \hat{\mathbf{Y}}_{o,S})$ 
14:     $\hat{\mathbf{J}}_{R \times S} \leftarrow \partial_S \Delta\hat{\mathbf{I}}_R(\hat{\mathbf{I}}_S, \hat{\mathbf{V}}_R, \mathbf{S}_\sigma, \hat{\mathbf{Y}}_{o,R})$ 
15:     $\hat{\mathbf{J}}_{R \times R} \leftarrow \partial_R \Delta\hat{\mathbf{I}}_R(\hat{\mathbf{I}}_S, \hat{\mathbf{V}}_R, \mathbf{S}_\sigma, \hat{\mathbf{Y}}_{o,R})$ 
16:    # Newton-Raphson iteration
17:    
$$\begin{bmatrix} \Delta\hat{\mathbf{I}}_S \\ \Delta\hat{\mathbf{V}}_R \end{bmatrix} \leftarrow \begin{bmatrix} \hat{\mathbf{J}}_{S \times S} & \hat{\mathbf{J}}_{S \times R} \\ \hat{\mathbf{J}}_{R \times S} & \hat{\mathbf{J}}_{R \times R} \end{bmatrix}^{-1} \begin{bmatrix} \Delta\hat{\mathbf{V}}_S \\ \Delta\hat{\mathbf{I}}_R \end{bmatrix}$$

18:    
$$\begin{bmatrix} \hat{\mathbf{I}}_S \\ \hat{\mathbf{V}}_R \end{bmatrix} \leftarrow \begin{bmatrix} \hat{\mathbf{I}}_S \\ \hat{\mathbf{V}}_R \end{bmatrix} - \begin{bmatrix} \Delta\hat{\mathbf{I}}_S \\ \Delta\hat{\mathbf{V}}_R \end{bmatrix}$$

19:    # Update
20:     $\hat{\mathbf{Y}}_{o,s} \leftarrow \hat{\mathbf{T}}_{o,s} \hat{\mathbf{Y}}_s \quad \forall s \in \mathcal{S}$ 
21:     $\hat{\mathbf{Y}}_{o,r} \leftarrow \hat{\mathbf{T}}_{o,r} \hat{\mathbf{Y}}_r \quad \forall r \in \mathcal{R}$ 
22:  end while
23: end procedure

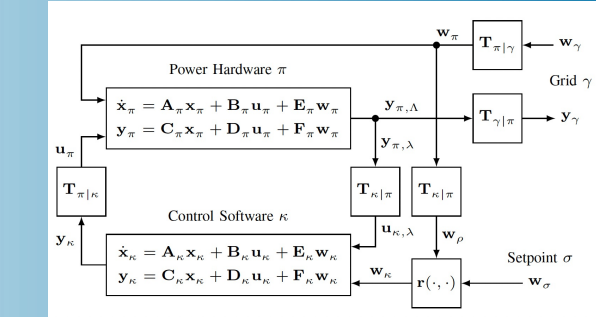
```

Part 2 – CIDER Models, Code & Examples

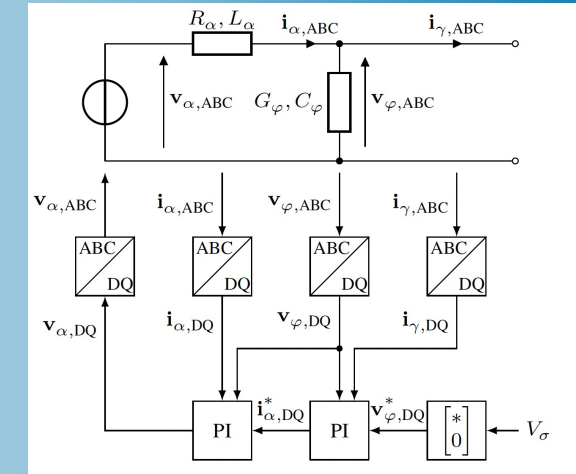
Detailed CIDER Models - Overview

- In Part 1 of this tutorial it was shown how the LTP models and functions of a generic CIDER are transformed to harmonic domain and ultimately employed in the HPF study.
- In this part: Derivation of specific CIDER models.
- Functions describing the external and internal transformations.
- Equations describing standard components of a CIDER:
 - Filter stages associated to the power hardware.
 - Controller stages associated to the control software.
- Combination of standard components to form the LTP models of CIDER's power hardware and control software.
- The derivation of the following CIDER models is shown in detail:
 - A simplistic grid-forming CIDER [12].
 - The nonlinear control law of a simplistic grid-following CIDER [12].
 - The linearization of the internal response of a grid-following CIDER including AC/DC interactions [18].
 - The linearization of the internal response of a grid-following CIDER including the dynamics of a PLL [19].

Generic structure of a CIDER:



Schematics of a grid-forming CIDER:



Circuit Configurations and Reference Frames

Assuming π and κ are modelled in ABC coordinates and DQ components, respectively.

Internal transform - $\tau_{\pi|\kappa}$ & $\tau_{\kappa|\pi}$:

- Park (DQ) transformation:

$$\mathbf{T}_{\kappa|\pi} = \mathbf{T}_{\pi|\kappa}^T, \mathbf{T}_{\pi|\kappa} = \sqrt{\frac{2}{3}} \begin{bmatrix} \cos(\theta(t)) & -\sin(\theta(t)) \\ \cos(\theta(t) - \frac{2\pi}{3}) & -\sin(\theta(t) - \frac{2\pi}{3}) \\ \cos(\theta(t) + \frac{2\pi}{3}) & -\sin(\theta(t) + \frac{2\pi}{3}) \end{bmatrix}$$

- Reference angle for transformation:

➤ Assumption: Synchronized to f_1 and exhibits a known offset θ_0 .

$$\theta(t) = 2\pi f_1 t + \theta_0$$

- Fourier coefficients, with $\alpha = \exp(j\frac{2\pi}{3})$:

$$\mathbf{T}_{\pi|\kappa,+1} = \sqrt{\frac{2}{3}} \exp(j\theta_0) \begin{bmatrix} \frac{1}{2} & -\frac{1}{2j} \\ \frac{1}{2}\alpha^* & -\frac{1}{2j}\alpha^* \\ \frac{1}{2}\alpha & -\frac{1}{2j}\alpha \end{bmatrix}, \mathbf{T}_{\pi|\kappa,-1} = \mathbf{T}_{\pi|\kappa,+1}^*$$

- Toeplitz matrix of $\mathbf{T}_{\pi|\kappa}$:

• Band structure, only Fourier coefficients at $h = \pm 1$ are nonzero.
 ➤ Introduces coupling between harmonics.

$$\widehat{\mathbf{T}}_{\pi|\kappa} = \begin{bmatrix} \ddots & \ddots & & & \\ \ddots & \mathbf{0} & \mathbf{T}_{\pi|\kappa,-1} & & \\ & \mathbf{T}_{\pi|\kappa,+1} & \mathbf{0} & \mathbf{T}_{\pi|\kappa,-1} & \\ & & \mathbf{T}_{\pi|\kappa,+1} & \mathbf{0} & \ddots \\ & & & \ddots & \ddots \end{bmatrix}$$

Circuit Configurations and Reference Frames

External transform - $\tau_{\pi|\gamma}$ & $\tau_{\gamma|\pi}$:

- Four-wire CIDER (with neutral leg) connected to four-wire grid:
 - All sequences (positive, negative and homopolar) can flow.
- Three-wire CIDER connected to four-wire grid:
 - Homopolar sequences are blocked in both directions.
- Toeplitz matrix of $\mathbf{T}_{\pi|\gamma}$:
 - Block-diagonal matrix, since in both cases only the Fourier coefficients at $h = 0$ are nonzero.

$$\mathbf{T}_{\pi|\gamma} = \mathbf{T}_{\gamma|\pi} = \text{diag}(\mathbf{1}_3)$$

$$\mathbf{T}_{\pi|\gamma} = \mathbf{T}_{\gamma|\pi} = \text{diag}(\mathbf{1}_3) - \frac{1}{3} \mathbf{1}_{3 \times 3}$$

$$\widehat{\mathbf{T}}_{\pi|\gamma} = \begin{bmatrix} \ddots & \ddots & & \\ \ddots & \mathbf{T}_{\pi|\gamma,0} & \mathbf{0} & \\ & \mathbf{0} & \mathbf{T}_{\pi|\gamma,0} & \mathbf{0} \\ & & \mathbf{0} & \mathbf{T}_{\pi|\gamma,0} \\ & & & \ddots & \ddots \end{bmatrix}$$

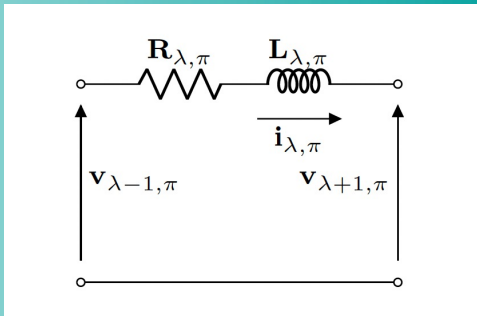
Standard Components: Filter Stage

- Filter stage λ in reference frame of the power hardware π :

- The power hardware is usually described in ABC coordinates.
- The filter stages are described by the dynamic equations of their equivalent circuits, as shown below.

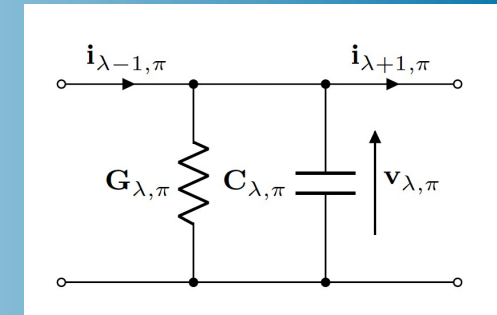
- Inductive stage:

$$\mathbf{v}_{\lambda-1,\pi}(t) - \mathbf{v}_{\lambda+1,\pi}(t) = \mathbf{R}_{\lambda,\pi} \mathbf{i}_{\lambda,\pi}(t) + \mathbf{L}_{\lambda,\pi} \frac{d}{dt} \mathbf{i}_{\lambda,\pi}(t)$$



- Capacitive stage:

$$\mathbf{i}_{\lambda-1,\pi}(t) - \mathbf{i}_{\lambda+1,\pi}(t) = \mathbf{G}_{\lambda,\pi} \mathbf{v}_{\lambda,\pi}(t) + \mathbf{C}_{\lambda,\pi} \frac{d}{dt} \mathbf{v}_{\lambda,\pi}(t)$$

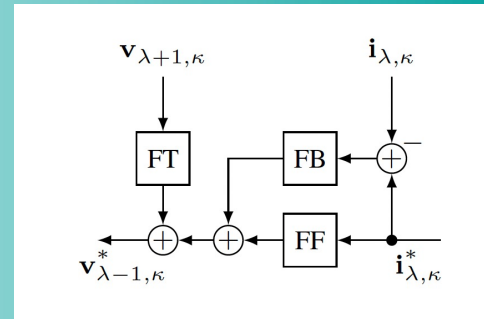


Standard Components: Controller Stage

- Controller stages λ in reference frame of the control software κ :
 - Consists of the Feed-Back (FB), Feed-Forward (FF) and the Feed-Through(FT) control.

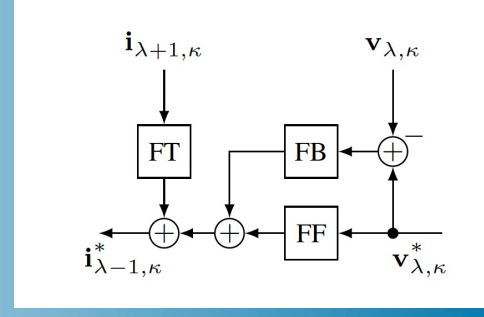
- Inductive stage:

$$\begin{aligned} \mathbf{v}_{\lambda-1,\kappa}^*(t) &= \mathbf{K}_{FB,\lambda} \left(\Delta \mathbf{i}_{\lambda,\kappa}(t) + \frac{1}{T_{FB,\lambda}} \int \Delta \mathbf{i}_{\lambda,\kappa}(t) dt \right) \\ &\quad + \mathbf{K}_{FF,\lambda} \mathbf{i}_{\lambda,\kappa}^*(t) + \mathbf{K}_{FT,\lambda} \mathbf{v}_{\lambda+1,\kappa}(t), \\ \Delta \mathbf{i}_{\lambda,\kappa}(t) &:= \mathbf{i}_{\lambda,\kappa}^*(t) - \mathbf{i}_{\lambda,\kappa}(t) \end{aligned}$$



- Capacitive stage:

$$\begin{aligned} \mathbf{i}_{\lambda-1,\kappa}^*(t) &= \mathbf{K}_{FB,\lambda} \left(\Delta \mathbf{v}_{\lambda,\kappa}(t) + \frac{1}{T_{FB,\lambda}} \int \Delta \mathbf{v}_{\lambda,\kappa}(t) dt \right) \\ &\quad + \mathbf{K}_{FF,\lambda} \mathbf{v}_{\lambda,\kappa}^*(t) + \mathbf{K}_{FT,\lambda} \mathbf{i}_{\lambda+1,\kappa}(t), \\ \Delta \mathbf{v}_{\lambda,\kappa}(t) &:= \mathbf{v}_{\lambda,\kappa}^*(t) - \mathbf{v}_{\lambda,\kappa}(t) \end{aligned}$$

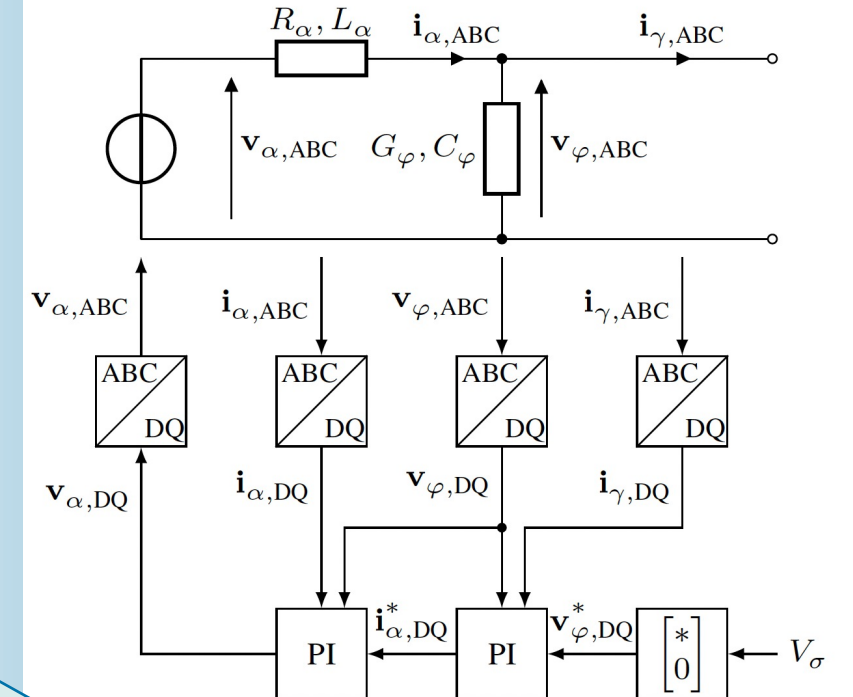


Where $\mathbf{K}_{(\cdot)}$ are the respective gains, and T_{FB} the time constant of the PI-controller.

Grid-Forming CIDER – PWM_LC_PI_Vf

Further explanations and detailed derivation in [12].

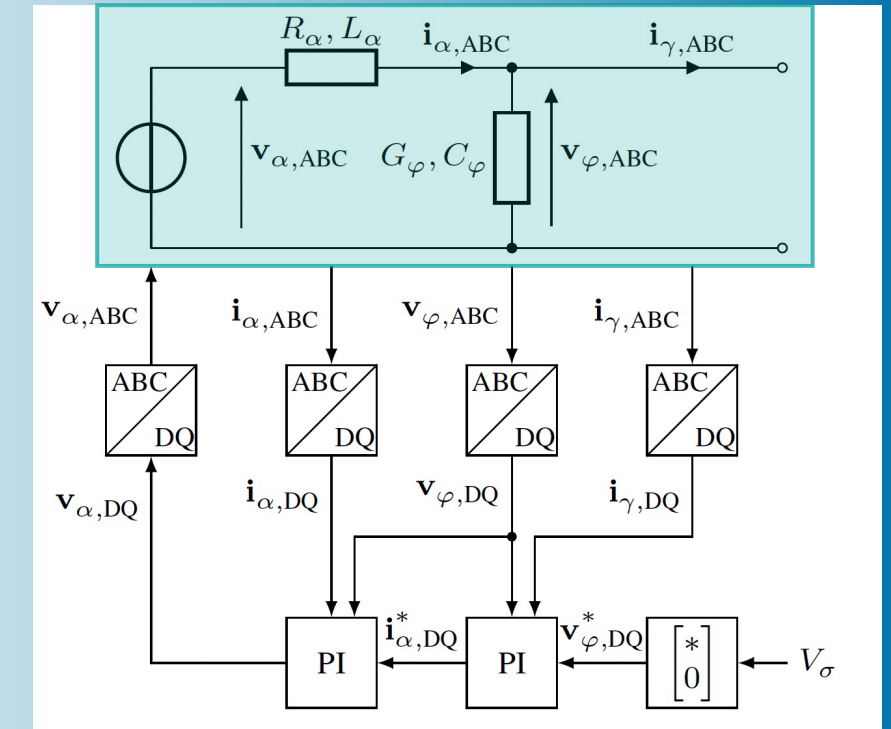
- Power hardware:
 - Actuator: 4-Leg PWM converter.
 - Assumption: Reference is perfectly tracked $\rightarrow \mathbf{v}_\alpha^*(t) = \mathbf{v}_\alpha(t)$.
 - Filter stages: LC filter.
- Transformations (Toeplitz matrices as previously introduced):
 - Internal transformation: Park.
 - External transformation: 4-leg converter to 4-wire system.
- Control software:
 - Controller stages: one per filter stage, PI control.
- Reference calculation:
 - Harmonic vector $\hat{\mathbf{V}}_{\varphi,DQ}^* = \text{col}_{h \in \mathcal{H}}(V_{\varphi,DQ,h}^*)$ consists of all zero elements except $V_{\varphi,D,0}^* = |V_\sigma|$.



Next step: Derivation of power hardware and control software LTP models based on the filter and controller stage equations previously introduced.

Grid-Forming CIDER – PWM_LC_PI_Vf

Power hardware:

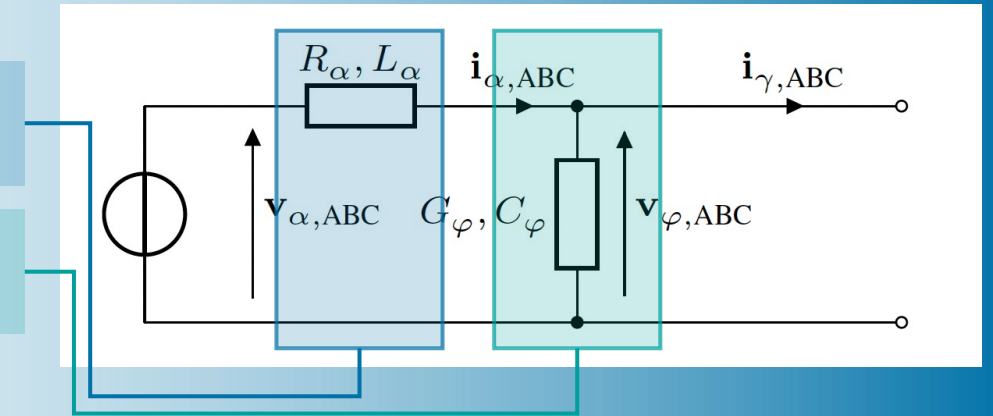


Grid-Forming CIDER – PWM_LC_PI_Vf

Power hardware:

$$\frac{d}{dt} \mathbf{i}_{\alpha,ABC}(t) = -\mathbf{L}_{\alpha,ABC}^{-1} \mathbf{R}_{\alpha,ABC} \mathbf{i}_{\alpha,ABC}(t) + \mathbf{L}_{\alpha,ABC}^{-1} \mathbf{v}_{\alpha,ABC}(t) - \mathbf{L}_{\alpha,ABC}^{-1} \mathbf{v}_{\varphi,ABC}(t)$$

$$\frac{d}{dt} \mathbf{v}_{\varphi,ABC}(t) = -\mathbf{C}_{\varphi,ABC}^{-1} \mathbf{G}_{\varphi,ABC} \mathbf{v}_{\varphi,ABC}(t) + \mathbf{C}_{\varphi,ABC}^{-1} \mathbf{i}_{\alpha,ABC}(t) - \mathbf{C}_{\varphi,ABC}^{-1} \mathbf{i}_{\gamma,ABC}(t)$$



Grid-Forming CIDER – PWM_LC_PI_Vf

Power hardware:

$$\frac{d}{dt} \mathbf{i}_{\alpha,ABC}(t) = -\mathbf{L}_{\alpha,ABC}^{-1} \mathbf{R}_{\alpha,ABC} \mathbf{i}_{\alpha,ABC}(t) + \mathbf{L}_{\alpha,ABC}^{-1} \mathbf{v}_{\alpha,ABC}(t) - \mathbf{L}_{\alpha,ABC}^{-1} \mathbf{v}_{\varphi,ABC}(t)$$

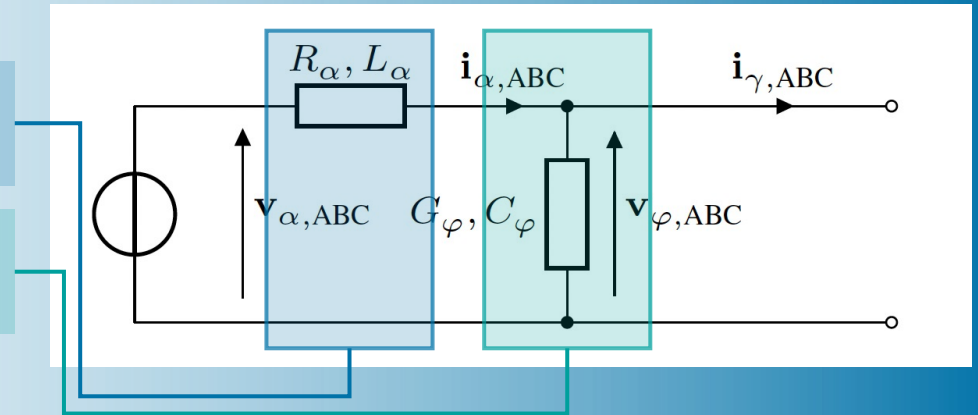
$$\frac{d}{dt} \mathbf{v}_{\varphi,ABC}(t) = -\mathbf{C}_{\varphi,ABC}^{-1} \mathbf{G}_{\varphi,ABC} \mathbf{v}_{\varphi,ABC}(t) + \mathbf{C}_{\varphi,ABC}^{-1} \mathbf{i}_{\alpha,ABC}(t) - \mathbf{C}_{\varphi,ABC}^{-1} \mathbf{i}_{\gamma,ABC}(t)$$

$$\mathbf{x}_\pi(t) = \begin{bmatrix} \mathbf{i}_{\alpha,ABC}(t) \\ \mathbf{v}_{\varphi,ABC}(t) \end{bmatrix}$$

$$\mathbf{u}_\pi(t) = \mathbf{v}_{\alpha,ABC}(t)$$

$$\mathbf{w}_\pi(t) = \mathbf{i}_{\gamma,ABC}(t)$$

$$\mathbf{y}_\pi(t) = \begin{bmatrix} \mathbf{x}_\pi(t) \\ \mathbf{w}_\pi(t) \end{bmatrix}$$

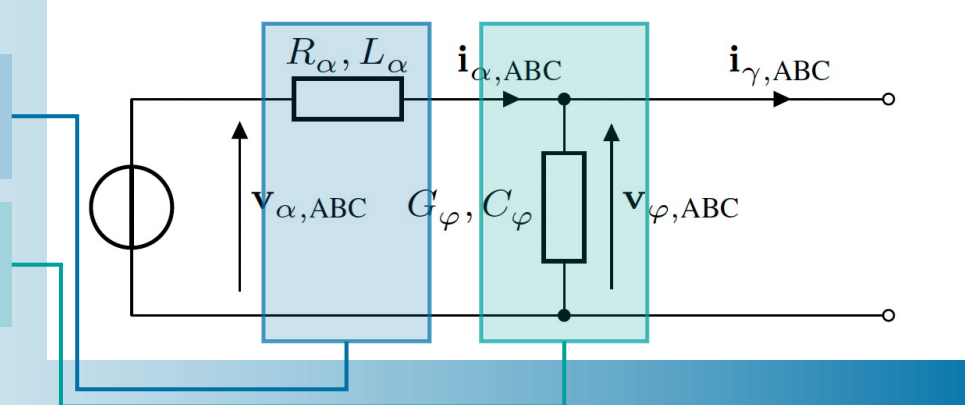


Grid-Forming CIDER – PWM_LC_PI_Vf

Power hardware:

$$\frac{d}{dt} \mathbf{i}_{\alpha,ABC}(t) = -\mathbf{L}_{\alpha,ABC}^{-1} \mathbf{R}_{\alpha,ABC} \mathbf{i}_{\alpha,ABC}(t) + \mathbf{L}_{\alpha,ABC}^{-1} \mathbf{v}_{\alpha,ABC}(t) - \mathbf{L}_{\alpha,ABC}^{-1} \mathbf{v}_{\varphi,ABC}(t)$$

$$\frac{d}{dt} \mathbf{v}_{\varphi,ABC}(t) = -\mathbf{C}_{\varphi,ABC}^{-1} \mathbf{G}_{\varphi,ABC} \mathbf{v}_{\varphi,ABC}(t) + \mathbf{C}_{\varphi,ABC}^{-1} \mathbf{i}_{\alpha,ABC}(t) - \mathbf{C}_{\varphi,ABC}^{-1} \mathbf{i}_{\gamma,ABC}(t)$$



State equation:

$$\begin{bmatrix} \dot{\mathbf{x}}_{\pi,1}(t) \\ \dot{\mathbf{x}}_{\pi,2}(t) \end{bmatrix} = \underbrace{\begin{bmatrix} -\mathbf{L}_{\alpha,ABC}^{-1} \mathbf{R}_{\alpha,ABC} & \mathbf{L}_{\alpha,ABC}^{-1} \\ \mathbf{C}_{\varphi,ABC}^{-1} & -\mathbf{C}_{\varphi,ABC}^{-1} \mathbf{G}_{\varphi,ABC} \end{bmatrix}}_{\mathbf{A}_{\pi}(t)} \begin{bmatrix} \mathbf{x}_{\pi,1}(t) \\ \mathbf{x}_{\pi,2}(t) \end{bmatrix} + \underbrace{\begin{bmatrix} \mathbf{L}_{\alpha,ABC}^{-1} \\ \mathbf{0}_{3 \times 3} \end{bmatrix}}_{\mathbf{B}_{\pi}(t)} \mathbf{u}_{\pi}(t) + \underbrace{\begin{bmatrix} \mathbf{0}_{3 \times 3} \\ -\mathbf{C}_{\varphi,ABC}^{-1} \end{bmatrix}}_{\mathbf{E}_{\pi}(t)} \mathbf{w}_{\pi}(t)$$

$$\mathbf{x}_{\pi}(t) = \begin{bmatrix} \mathbf{i}_{\alpha,ABC}(t) \\ \mathbf{v}_{\varphi,ABC}(t) \end{bmatrix}$$

$$\mathbf{u}_{\pi}(t) = \mathbf{v}_{\alpha,ABC}(t)$$

$$\mathbf{w}_{\pi}(t) = \mathbf{i}_{\gamma,ABC}(t)$$

$$\mathbf{y}_{\pi}(t) = \begin{bmatrix} \mathbf{x}_{\pi}(t) \\ \mathbf{w}_{\pi}(t) \end{bmatrix}$$

Output equation:

$$\begin{bmatrix} \mathbf{x}_{\pi}(t) \\ \mathbf{w}_{\pi}(t) \end{bmatrix} = \underbrace{\begin{bmatrix} \text{diag}(\mathbf{1}_6) \\ \mathbf{0}_{3 \times 6} \end{bmatrix}}_{\mathbf{C}_{\pi}(t)} \mathbf{x}_{\pi}(t) + \underbrace{\begin{bmatrix} \mathbf{0}_{6 \times 3} \\ \mathbf{0}_{3 \times 3} \end{bmatrix}}_{\mathbf{D}_{\pi}(t)} \mathbf{u}_{\pi}(t) + \underbrace{\begin{bmatrix} \mathbf{0}_{6 \times 3} \\ \text{diag}(\mathbf{1}_3) \end{bmatrix}}_{\mathbf{F}_{\pi}(t)} \mathbf{w}_{\pi}(t)$$

Grid-Forming CIDER – PWM_LC_PI_Vf

Power hardware:

All matrices are constant → They are fully described by their Fourier coefficients at $h = 0$.

$$\mathbf{A}_\pi(t) = \sum_h \mathbf{A}_{\pi,h} \exp(j h 2\pi f_1 t) = \mathbf{A}_{\pi,0}$$

→ The matrices of the power hardware model in harmonic domain will exhibit a block-diagonal structure.

$$\widehat{\mathbf{A}}_\pi = \begin{bmatrix} \ddots & \ddots & & \\ \ddots & \mathbf{A}_{\pi,0} & \mathbf{0} & \\ \mathbf{0} & \mathbf{A}_{\pi,0} & \mathbf{0} & \\ \mathbf{0} & \mathbf{0} & \mathbf{A}_{\pi,0} & \\ & & & \ddots \end{bmatrix}$$

$$\mathbf{x}_\pi(t) = \begin{bmatrix} \mathbf{i}_{\alpha,\text{ABC}}(t) \\ \mathbf{v}_{\varphi,\text{ABC}}(t) \end{bmatrix}$$

$$\mathbf{u}_\pi(t) = \mathbf{v}_{\alpha,\text{ABC}}(t)$$

$$\mathbf{w}_\pi(t) = \mathbf{i}_{\gamma,\text{ABC}}(t)$$

$$\mathbf{y}_\pi(t) = \begin{bmatrix} \mathbf{x}_\pi(t) \\ \mathbf{w}_\pi(t) \end{bmatrix}$$

State equation:

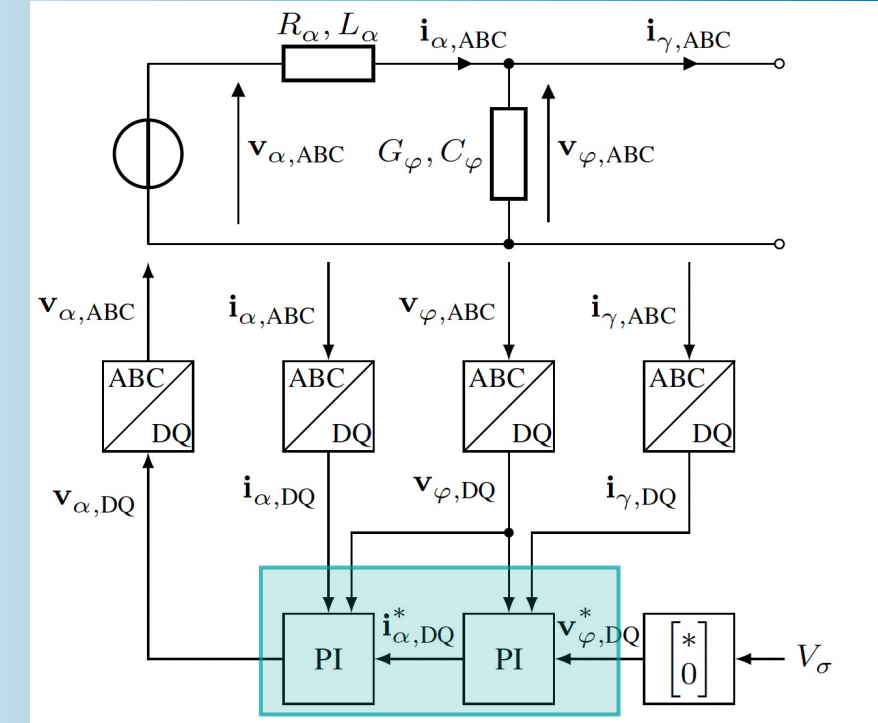
$$\begin{bmatrix} \dot{\mathbf{x}}_{\pi,1}(t) \\ \dot{\mathbf{x}}_{\pi,2}(t) \end{bmatrix} = \underbrace{\begin{bmatrix} -\mathbf{L}_{\alpha,\text{ABC}}^{-1} \mathbf{R}_{\alpha,\text{ABC}} & \mathbf{L}_{\alpha,\text{ABC}}^{-1} \\ \mathbf{C}_{\varphi,\text{ABC}}^{-1} & -\mathbf{C}_{\varphi,\text{ABC}}^{-1} \mathbf{G}_{\varphi,\text{ABC}} \end{bmatrix}}_{\mathbf{A}_\pi(t)} \begin{bmatrix} \mathbf{x}_{\pi,1}(t) \\ \mathbf{x}_{\pi,2}(t) \end{bmatrix} + \underbrace{\begin{bmatrix} \mathbf{L}_{\alpha,\text{ABC}}^{-1} \\ \mathbf{0}_{3 \times 3} \end{bmatrix}}_{\mathbf{B}_\pi(t)} \mathbf{u}_\pi(t) + \underbrace{\begin{bmatrix} \mathbf{0}_{3 \times 3} \\ -\mathbf{C}_{\varphi,\text{ABC}}^{-1} \end{bmatrix}}_{\mathbf{E}_\pi(t)} \mathbf{w}_\pi(t)$$

Output equation:

$$\begin{bmatrix} \mathbf{x}_\pi(t) \\ \mathbf{w}_\pi(t) \end{bmatrix} = \underbrace{\begin{bmatrix} \text{diag}(\mathbf{1}_6) \\ \mathbf{0}_{3 \times 6} \end{bmatrix}}_{\mathbf{C}_\pi(t)} \mathbf{x}_\pi(t) + \underbrace{\begin{bmatrix} \mathbf{0}_{6 \times 3} \\ \mathbf{0}_{3 \times 3} \end{bmatrix}}_{\mathbf{D}_\pi(t)} \mathbf{u}_\pi(t) + \underbrace{\begin{bmatrix} \mathbf{0}_{6 \times 3} \\ \text{diag}(\mathbf{1}_3) \end{bmatrix}}_{\mathbf{F}_\pi(t)} \mathbf{w}_\pi(t)$$

Grid-Forming CIDER – PWM_LC_PI_Vf

Control software:



Grid-Forming CIDER – PWM_LC_PI_Vf

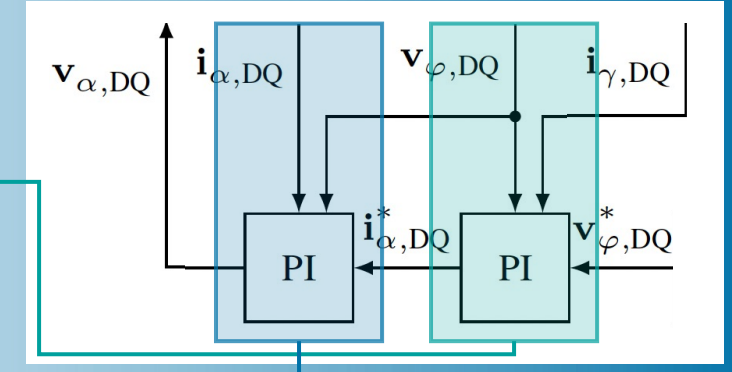
Control software:

$$\mathbf{i}_{\alpha,DQ}^*(t) = \mathbf{K}_{FB,\varphi} \left(\Delta \mathbf{v}_{\varphi,DQ}(t) + \frac{1}{T_{FB,\varphi}} \int \Delta \mathbf{v}_{\varphi,DQ}(t) dt \right) + \mathbf{K}_{FT,\varphi} \mathbf{i}_{\gamma,DQ}(t) + \mathbf{K}_{FF,\varphi} \mathbf{v}_{\varphi,DQ}^*(t)$$

$$\Delta \mathbf{v}_{\varphi,DQ}(t) := \mathbf{v}_{\varphi,DQ}^*(t) - \mathbf{v}_{\varphi,DQ}(t)$$

$$\mathbf{v}_{\alpha,DQ}^*(t) = \mathbf{K}_{FB,\alpha} \left(\Delta \mathbf{i}_{\alpha,DQ}(t) + \frac{1}{T_{FB,\alpha}} \int \Delta \mathbf{i}_{\alpha,DQ}(t) dt \right) + \mathbf{K}_{FT,\alpha} \mathbf{v}_{\varphi,DQ}(t) + \mathbf{K}_{FF,\alpha} \mathbf{i}_{\alpha,DQ}^*(t)$$

$$\Delta \mathbf{i}_{\alpha,DQ}(t) := \mathbf{i}_{\alpha,DQ}^*(t) - \mathbf{i}_{\alpha,DQ}(t)$$



Grid-Forming CIDER – PWM_LC_PI_Vf

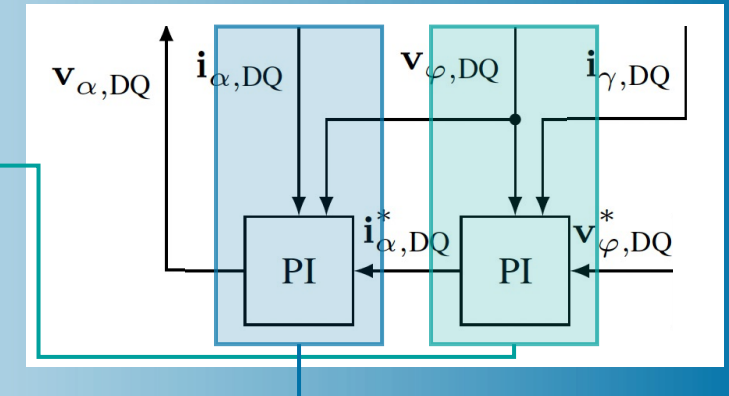
Control software:

$$\mathbf{i}_{\alpha,DQ}^*(t) = \frac{\mathbf{K}_{FB,\varphi}}{T_{FB,\varphi}} \int \Delta \mathbf{v}_{\varphi,DQ}(t) dt - \mathbf{K}_{FB,\varphi} \mathbf{v}_{\varphi,DQ}(t) + \mathbf{K}_{FT,\varphi} \mathbf{i}_{\gamma,DQ}(t) + (\mathbf{K}_{FF,\varphi} + \mathbf{K}_{FB,\varphi}) \mathbf{v}_{\varphi,DQ}^*(t)$$

$$\Delta \mathbf{v}_{\varphi,DQ}(t) := \mathbf{v}_{\varphi,DQ}^*(t) - \mathbf{v}_{\varphi,DQ}(t)$$

$$\mathbf{v}_{\alpha,DQ}^*(t) = \frac{\mathbf{K}_{FB,\alpha}}{T_{FB,\alpha}} \int \Delta \mathbf{i}_{\alpha,DQ}(t) dt - \mathbf{K}_{FB,\alpha} \mathbf{i}_{\alpha,DQ}(t) + \mathbf{K}_{FT,\alpha} \mathbf{v}_{\varphi,DQ}(t) + (\mathbf{K}_{FF,\alpha} + \mathbf{K}_{FB,\alpha}) \mathbf{i}_{\alpha,DQ}^*(t)$$

$$\Delta \mathbf{i}_{\alpha,DQ}(t) := \mathbf{i}_{\alpha,DQ}^*(t) - \mathbf{i}_{\alpha,DQ}(t)$$



$$\mathbf{x}_\kappa(t) = \begin{bmatrix} \Delta \mathbf{i}_{\alpha,DQ}(t) \\ \Delta \mathbf{v}_{\varphi,DQ}(t) \end{bmatrix} dt$$

$$\mathbf{u}_\kappa(t) = \begin{bmatrix} \mathbf{i}_{\alpha,DQ}(t) \\ \mathbf{v}_{\varphi,DQ}(t) \\ \mathbf{i}_{\gamma,DQ}(t) \end{bmatrix}$$

$$\mathbf{w}_\kappa(t) = \mathbf{v}_{\varphi,DQ}^*(t)$$

$$\mathbf{y}_\kappa(t) = \mathbf{v}_{\alpha,DQ}^*(t)$$

Grid-Forming CIDER – PWM_LC_PI_Vf

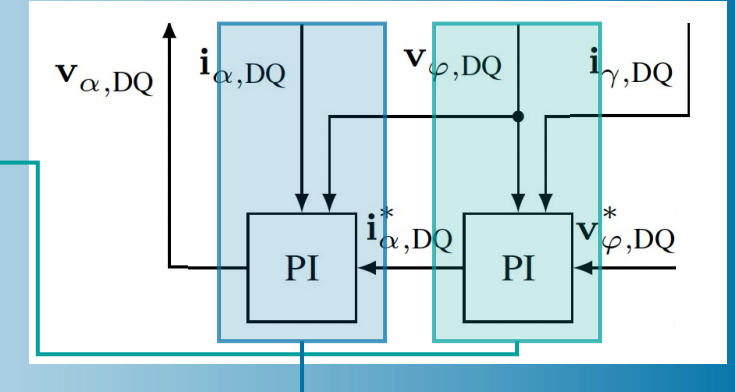
Control software:

$$\mathbf{i}_{\alpha,DQ}^*(t) = \frac{\mathbf{K}_{FB,\varphi}}{T_{FB,\varphi}} \mathbf{x}_{\kappa,2}(t) - \mathbf{K}_{FB,\varphi} \mathbf{u}_{\kappa,2}(t) + \mathbf{K}_{FT,\varphi} \mathbf{u}_{\kappa,3}(t) + (\mathbf{K}_{FF,\varphi} + \mathbf{K}_{FB,\varphi}) \mathbf{w}_{\kappa}(t)$$

$$\Delta \mathbf{v}_{\varphi,DQ}(t) := \mathbf{w}_{\kappa}(t) - \mathbf{u}_{\kappa,2}(t)$$

$$\mathbf{y}_{\kappa}(t) = \frac{\mathbf{K}_{FB,\alpha}}{T_{FB,\alpha}} \mathbf{x}_{\kappa,1}(t) - \mathbf{K}_{FB,\alpha} \mathbf{u}_{\kappa,1}(t) + \mathbf{K}_{FT,\alpha} \mathbf{u}_{\kappa,2}(t) + (\mathbf{K}_{FF,\alpha} + \mathbf{K}_{FB,\alpha}) \mathbf{i}_{\alpha,DQ}^*(t)$$

$$\Delta \mathbf{i}_{\alpha,DQ}(t) := \mathbf{i}_{\alpha,DQ}^*(t) - \mathbf{u}_{\kappa,1}(t)$$



$$\mathbf{x}_{\kappa}(t) = \int \begin{bmatrix} \Delta \mathbf{i}_{\alpha,DQ}(t) \\ \Delta \mathbf{v}_{\varphi,DQ}(t) \end{bmatrix} dt$$

$$\mathbf{u}_{\kappa}(t) = \begin{bmatrix} \mathbf{i}_{\alpha,DQ}(t) \\ \mathbf{v}_{\varphi,DQ}(t) \\ \mathbf{i}_{\gamma,DQ}(t) \end{bmatrix}$$

$$\mathbf{w}_{\kappa}(t) = \mathbf{v}_{\varphi,DQ}^*(t)$$

$$\mathbf{y}_{\kappa}(t) = \mathbf{v}_{\alpha,DQ}^*(t)$$

Grid-Forming CIDER – PWM_LC_PI_Vf

Control software:

$$\mathbf{i}_{\alpha,DQ}^*(t) = \frac{\mathbf{K}_{FB,\varphi}}{T_{FB,\varphi}} \mathbf{x}_{\kappa,2}(t) - \mathbf{K}_{FB,\varphi} \mathbf{u}_{\kappa,2}(t) + \mathbf{K}_{FT,\varphi} \mathbf{u}_{\kappa,3}(t) + (\mathbf{K}_{FF,\varphi} + \mathbf{K}_{FB,\varphi}) \mathbf{w}_{\kappa}(t)$$

$$\Delta \mathbf{v}_{\varphi,DQ}(t) := \mathbf{w}_{\kappa}(t) - \mathbf{u}_{\kappa,2}(t)$$

$$\mathbf{y}_{\kappa}(t) = \frac{\mathbf{K}_{FB,\alpha}}{T_{FB,\alpha}} \mathbf{x}_{\kappa,1}(t) - \mathbf{K}_{FB,\alpha} \mathbf{u}_{\kappa,1}(t) + \mathbf{K}_{FT,\alpha} \mathbf{u}_{\kappa,2}(t) + (\mathbf{K}_{FF,\alpha} + \mathbf{K}_{FB,\alpha}) \mathbf{i}_{\alpha,DQ}^*(t)$$

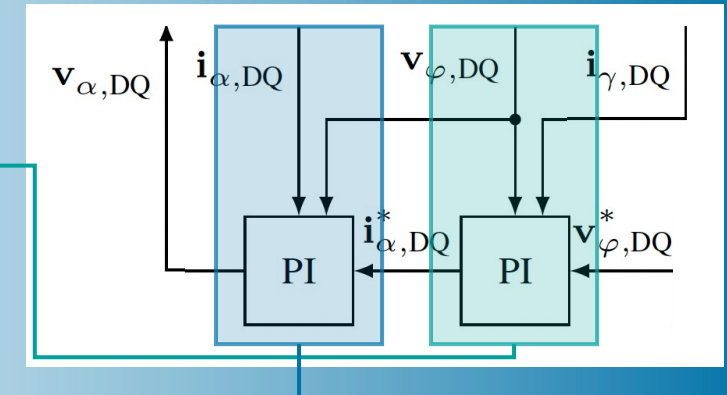
$$\Delta \mathbf{i}_{\alpha,DQ}(t) := \mathbf{i}_{\alpha,DQ}^*(t) - \mathbf{u}_{\kappa,1}(t)$$

State equation:

$$\begin{bmatrix} \dot{\mathbf{x}}_{\kappa,1}(t) \\ \dot{\mathbf{x}}_{\kappa,2}(t) \end{bmatrix} = \begin{bmatrix} \Delta \mathbf{i}_{\alpha,DQ}(t) \\ \Delta \mathbf{v}_{\varphi,DQ}(t) \end{bmatrix} = \begin{bmatrix} \mathbf{i}_{\alpha,DQ}^*(t) \\ \mathbf{v}_{\varphi,DQ}^*(t) \end{bmatrix} - \begin{bmatrix} \mathbf{i}_{\alpha,DQ}(t) \\ \mathbf{v}_{\varphi,DQ}(t) \end{bmatrix} = \begin{bmatrix} \mathbf{i}_{\alpha,DQ}^*(t) \\ \mathbf{w}_{\kappa}(t) \end{bmatrix} - \begin{bmatrix} \mathbf{u}_{\kappa,1}(t) \\ \mathbf{u}_{\kappa,2}(t) \end{bmatrix}$$

Output equation:

$$\mathbf{y}_{\kappa}(t) = \frac{\mathbf{K}_{FB,\alpha}}{T_{FB,\alpha}} \mathbf{x}_{\kappa,1}(t) - \mathbf{K}_{FB,\alpha} \mathbf{u}_{\kappa,1}(t) + \mathbf{K}_{FT,\alpha} \mathbf{u}_{\kappa,2}(t) + (\mathbf{K}_{FF,\alpha} + \mathbf{K}_{FB,\alpha}) \mathbf{i}_{\alpha,DQ}^*(t)$$



$$\mathbf{x}_{\kappa}(t) = \int \begin{bmatrix} \Delta \mathbf{i}_{\alpha,DQ}(t) \\ \Delta \mathbf{v}_{\varphi,DQ}(t) \end{bmatrix} dt$$

$$\mathbf{u}_{\kappa}(t) = \begin{bmatrix} \mathbf{i}_{\alpha,DQ}(t) \\ \mathbf{v}_{\varphi,DQ}(t) \\ \mathbf{i}_{\gamma,DQ}(t) \end{bmatrix}$$

$$\mathbf{w}_{\kappa}(t) = \mathbf{v}_{\varphi,DQ}^*(t)$$

$$\mathbf{y}_{\kappa}(t) = \mathbf{v}_{\alpha,DQ}^*(t)$$

Grid-Forming CIDER – PWM_LC_PI_Vf

Control software:

$$\mathbf{i}_{\alpha,DQ}^*(t) = \frac{\mathbf{K}_{FB,\varphi}}{T_{FB,\varphi}} \mathbf{x}_{\kappa,2}(t) - \mathbf{K}_{FB,\varphi} \mathbf{u}_{\kappa,2}(t) + \mathbf{K}_{FT,\varphi} \mathbf{u}_{\kappa,3}(t) + (\mathbf{K}_{FF,\varphi} + \mathbf{K}_{FB,\varphi}) \mathbf{w}_\kappa(t)$$

$$\Delta \mathbf{v}_{\varphi,DQ}(t) := \mathbf{w}_\kappa(t) - \mathbf{u}_{\kappa,2}(t)$$

$$\mathbf{y}_\kappa(t) = \frac{\mathbf{K}_{FB,\alpha}}{T_{FB,\alpha}} \mathbf{x}_{\kappa,1}(t) - \mathbf{K}_{FB,\alpha} \mathbf{u}_{\kappa,1}(t) + \mathbf{K}_{FT,\alpha} \mathbf{u}_{\kappa,2}(t) + (\mathbf{K}_{FF,\alpha} + \mathbf{K}_{FB,\alpha}) \mathbf{i}_{\alpha,DQ}^*(t)$$

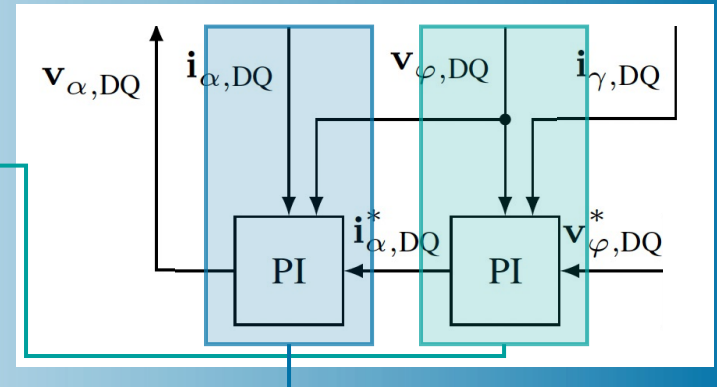
$$\Delta \mathbf{i}_{\alpha,DQ}(t) := \mathbf{i}_{\alpha,DQ}^*(t) - \mathbf{u}_{\kappa,1}(t)$$

State equation:

$$\begin{bmatrix} \dot{\mathbf{x}}_{\kappa,1}(t) \\ \dot{\mathbf{x}}_{\kappa,2}(t) \end{bmatrix} = \begin{bmatrix} \Delta \mathbf{i}_{\alpha,DQ}(t) \\ \Delta \mathbf{v}_{\varphi,DQ}(t) \end{bmatrix} = \begin{bmatrix} \mathbf{i}_{\alpha,DQ}^*(t) \\ \mathbf{v}_{\varphi,DQ}^*(t) \end{bmatrix} - \begin{bmatrix} \mathbf{i}_{\alpha,DQ}(t) \\ \mathbf{v}_{\varphi,DQ}(t) \end{bmatrix} = \begin{bmatrix} \mathbf{i}_{\alpha,DQ}^*(t) \\ \mathbf{w}_\kappa(t) \end{bmatrix} - \begin{bmatrix} \mathbf{u}_{\kappa,1}(t) \\ \mathbf{u}_{\kappa,2}(t) \end{bmatrix}$$

Output equation:

$$\mathbf{y}_\kappa(t) = \frac{\mathbf{K}_{FB,\alpha}}{T_{FB,\alpha}} \mathbf{x}_{\kappa,1}(t) - \mathbf{K}_{FB,\alpha} \mathbf{u}_{\kappa,1}(t) + \mathbf{K}_{FT,\alpha} \mathbf{u}_{\kappa,2}(t) + (\mathbf{K}_{FF,\alpha} + \mathbf{K}_{FB,\alpha}) \mathbf{i}_{\alpha,DQ}^*(t)$$



$$\mathbf{x}_\kappa(t) = \int \begin{bmatrix} \Delta \mathbf{i}_{\alpha,DQ}(t) \\ \Delta \mathbf{v}_{\varphi,DQ}(t) \end{bmatrix} dt$$

$$\mathbf{u}_\kappa(t) = \begin{bmatrix} \mathbf{i}_{\alpha,DQ}(t) \\ \mathbf{v}_{\varphi,DQ}(t) \\ \mathbf{i}_{\gamma,DQ}(t) \end{bmatrix}$$

$$\mathbf{w}_\kappa(t) = \mathbf{v}_{\varphi,DQ}^*(t)$$

$$\mathbf{y}_\kappa(t) = \mathbf{v}_{\alpha,DQ}^*(t)$$

Grid-Forming CIDER – PWM_LC_PI_Vf

Control software:

As before all parameters that enter the state-space matrices are constant → They are fully described by their Fourier coefficients at $h = 0$.

$$\mathbf{A}_\kappa(t) = \sum_h \mathbf{A}_{\kappa,h} \exp(j h 2\pi f_1 t) = \mathbf{A}_{\kappa,0}$$

→ The matrices of the control software model in harmonic domain will exhibit a block-diagonal structure.

State equation:

$$\begin{bmatrix} \dot{\mathbf{x}}_{\kappa,1}(t) \\ \dot{\mathbf{x}}_{\kappa,2}(t) \end{bmatrix} = \begin{bmatrix} \Delta \mathbf{i}_{\alpha,DQ}(t) \\ \Delta \mathbf{v}_{\varphi,DQ}(t) \end{bmatrix} = \begin{bmatrix} \mathbf{i}_{\alpha,DQ}^*(t) \\ \mathbf{v}_{\varphi,DQ}^*(t) \end{bmatrix} - \begin{bmatrix} \mathbf{i}_{\alpha,DQ}(t) \\ \mathbf{v}_{\varphi,DQ}(t) \end{bmatrix} - \begin{bmatrix} \mathbf{i}_{\alpha,DQ}^*(t) \\ \mathbf{w}_\kappa(t) \end{bmatrix} - \begin{bmatrix} \mathbf{u}_{\kappa,1}(t) \\ \mathbf{u}_{\kappa,2}(t) \end{bmatrix}$$

Output equation:

$$\mathbf{y}_\kappa(t) = \frac{\mathbf{K}_{FB,\alpha}}{T_{FB,\alpha}} \mathbf{x}_{\kappa,1}(t) - \mathbf{K}_{FB,\alpha} \mathbf{u}_{\kappa,1}(t) + \mathbf{K}_{FT,\alpha} \mathbf{u}_{\kappa,2}(t) + (\mathbf{K}_{FF,\alpha} + \mathbf{K}_{FB,\alpha}) \mathbf{i}_{\alpha,DQ}^*(t)$$

$$\widehat{\mathbf{A}}_\kappa = \begin{bmatrix} \ddots & \ddots & & & \\ \ddots & \mathbf{A}_{\kappa,0} & \mathbf{0} & & \\ & \mathbf{0} & \mathbf{A}_{\kappa,0} & \mathbf{0} & \\ & & \mathbf{0} & \mathbf{A}_{\kappa,0} & \\ & & & \ddots & \ddots \end{bmatrix}$$

$$\mathbf{x}_\kappa(t) = \int \begin{bmatrix} \Delta \mathbf{i}_{\alpha,DQ}(t) \\ \Delta \mathbf{v}_{\varphi,DQ}(t) \end{bmatrix} dt$$

$$\mathbf{u}_\kappa(t) = \begin{bmatrix} \mathbf{i}_{\alpha,DQ}(t) \\ \mathbf{v}_{\varphi,DQ}(t) \\ \mathbf{i}_{\gamma,DQ}(t) \end{bmatrix}$$

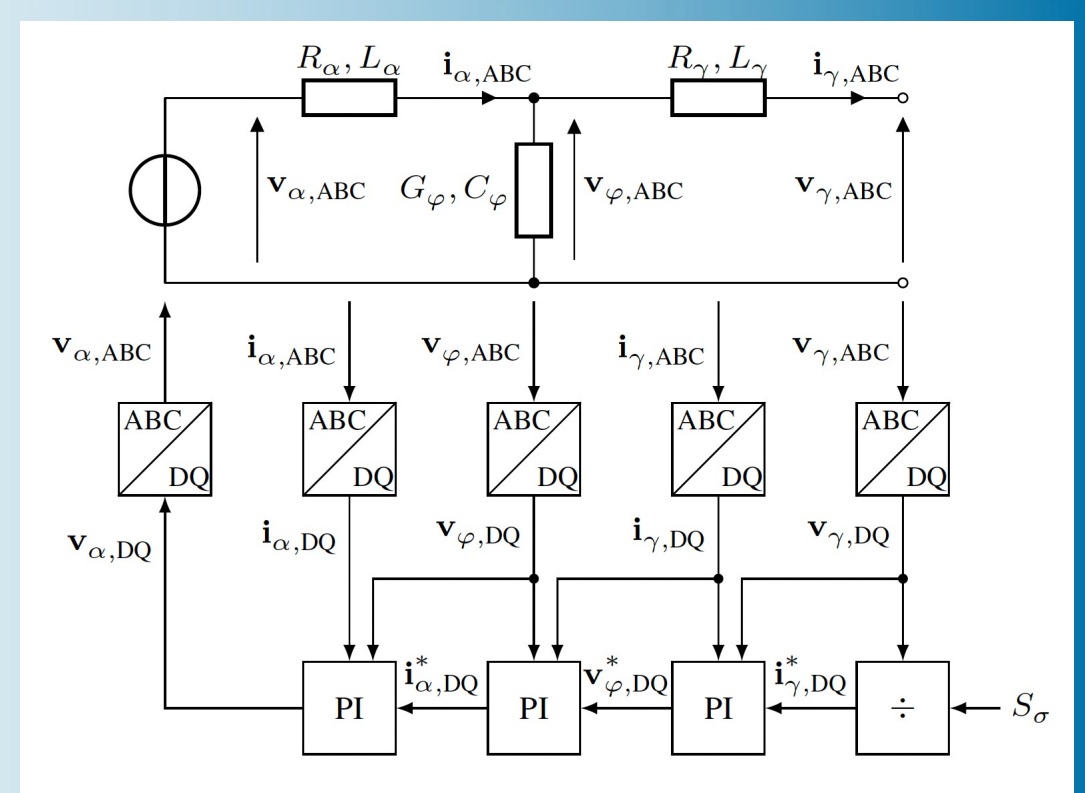
$$\mathbf{w}_\kappa(t) = \mathbf{v}_{\varphi,DQ}^*(t)$$

$$\mathbf{y}_\kappa(t) = \mathbf{v}_{\alpha,DQ}^*(t)$$

Grid-Following CIDER – PWM_LCL_PI_PQ

Further explanations and detailed derivation in [12].

- Power hardware:
 - Actuator: 3-Leg PWM converter
 - $\mathbf{v}_\alpha^*(t) = \mathbf{v}_\alpha(t)$.¹
 - Filter stages: LCL filter.¹
- Transformations (Toeplitz matrices as previously introduced):
 - Internal transformation: Park.
 - External transformation: 3-leg converter to 4-wire system.
- Control software:
 - Controller stages: one per filter stage, PI control.¹
- Reference calculation: Nonlinear.



Derivation shown in detail in the following.

¹Same procedure as for PWM_LC_PI_Vf

Grid-Following CIDER – PWM_LCL_PI_PQ

Reference calculation:

- Nonlinear time-domain expression:
 - Assumption 1: CIDER is perfectly aligned to the fundamental positive-sequence component of the grid voltage.
→ $v_{\gamma,Q}(t)$ can be omitted in the reference calculation.
- The Fourier coefficients of $\mathbf{i}_{\gamma,DQ}^*(t)$ are needed for the harmonic domain representation.
→ Exact expressions which relate the Fourier coefficients of the reciprocal $\frac{1}{v_{\gamma,D}(t)}$ with $v_{\gamma,D}(t)$ is complicated and computationally expensive to evaluate.

$$\mathbf{w}_k(t) = \mathbf{r}(\mathbf{w}_\rho(t), \mathbf{w}_\sigma(t))$$

↔

$$\mathbf{i}_{\gamma,DQ}^*(t) = \frac{1}{v_{\gamma,D}(t)} \begin{bmatrix} P_\sigma \\ Q_\sigma \end{bmatrix}$$

$$\begin{aligned} \mathbf{i}_{\gamma,DQ}^*(t) &= \frac{1}{v_{\gamma,D}(t)} \begin{bmatrix} P_\sigma \\ Q_\sigma \end{bmatrix} \\ &\approx \sum_h \Psi_h \exp(j h 2\pi f_1 t) \begin{bmatrix} P_\sigma \\ Q_\sigma \end{bmatrix} \end{aligned}$$

Grid-Following CIDER – PWM_LCL_PI_PQ

- $v_{\gamma,D}(t)$ can be rewritten using its time-variant signal content $\xi_D(t)$:
 - Assumption 2: The time-variant signal content of $v_{\gamma,D}(t)$ is small.
 - Taylor approximation of $1/(1 + x)$ can be used.
- Reciprocal of the grid voltage:
 - Approximated by a second-order Taylor series:

$$v_{\gamma,D}(t) = V_{\gamma,D,0}(1 + \xi_D(t)), \quad |\xi_D(t)| \ll 1$$

$$\xi_D(t) = \sum_{h \neq 0} \frac{V_{\gamma,D,h}}{V_{\gamma,D,0}} \exp(j h 2\pi f_1 t)$$

$$\begin{aligned} \frac{1}{v_{\gamma,D}(t)} &= \frac{1}{V_{\gamma,D,0}(1 + \xi_D(t))} \approx \frac{1}{V_{\gamma,D,0}} (1 - \xi_D(t) + \xi_D^2(t)) \\ &= \sum_h \Psi_h \exp(j h 2\pi f_1 t) \end{aligned}$$

- With Fourier Coefficients:

$$\begin{aligned} \mathbf{i}_{\gamma,DQ}^*(t) &= \frac{1}{v_{\gamma,D}(t)} \begin{bmatrix} P_\sigma \\ Q_\sigma \end{bmatrix} \\ &\approx \sum_h \Psi_h \exp(j h 2\pi f_1 t) \begin{bmatrix} P_\sigma \\ Q_\sigma \end{bmatrix} \end{aligned}$$

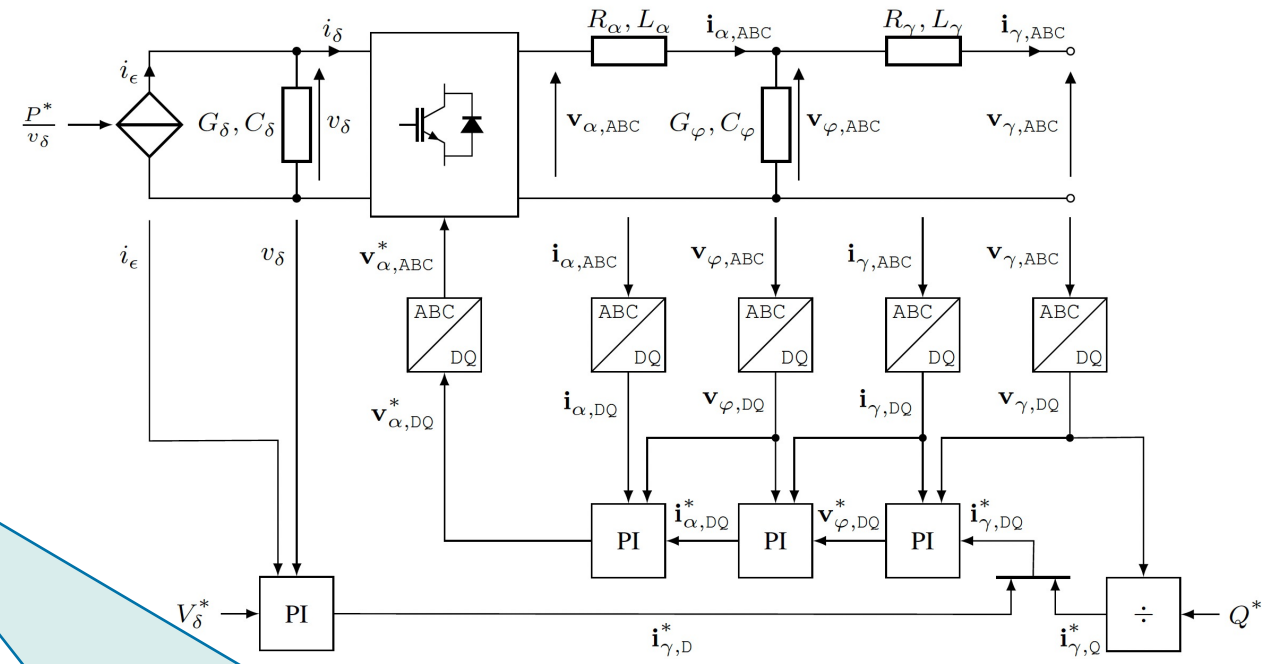
$$\Psi_h = \begin{cases} \frac{1}{V_{\gamma,D,0}} + \sum_{h \neq 0} \frac{|V_{\gamma,D,h}|^2}{V_{\gamma,D,0}^3} & h = 0 \\ -\frac{V_{\gamma,D,h}}{V_{\gamma,D,0}^2} + \sum_{i \neq 0} \frac{V_{\gamma,D,i} V_{\gamma,D,h-i}}{V_{\gamma,D,0}^3} & \text{otherwise} \end{cases}$$

Grid-Following CIDER – PWM_LCL_C_PI_VQ_I

Further explanations and detailed derivation in [18].

- Power hardware consists of:
 - AC filter stages.¹
 - Actuator → nonlinear.
 - DC filter stage.¹
 - DC equivalent current calculation → nonlinear.
- Control software:
 - AC controller stages.¹
 - DC controller stage.¹
- Reference calculation.¹

¹Same procedure as for PWM_LCL_PI_PQ



Nonlinearities within the internal response of the CIDER.
→ Linearization in time domain around time-periodic trajectories.

Grid-Following CIDER – PWM_LCL_C_PI_VQ_I

DC Equivalent Current Calculation:

- Nonlinear time-domain expression:

➤ Assumption 1: DC equivalent current is computed in order to track the power setpoint P^* .

➤ Assumption 2: DC voltage control tracks its reference without steady-state error.

➤ Assumption 3: DC voltage's time-variant content is low.

- DC equivalent current can be linearized around the DC voltage reference V_δ^* .

$$i_\epsilon(t) = \frac{P^*}{v_\delta(t)}$$

$$V_{\delta,0} = V_\delta^*$$

$$v_\delta(t) = V_{\delta,0}(1 + \xi(t)), \quad |\xi(t)| \ll 1$$

$$i_\epsilon(t) \approx \frac{P^*}{V_\delta^*} - \frac{P^*}{V_\delta^{*2}}(v_\delta(t) - V_\delta^*) = 2\frac{P^*}{V_\delta^*} - \frac{P^*}{V_\delta^{*2}}v_\delta(t)$$

Grid-Following CIDER – PWM_LCL_C_PI_VQ_I

Actuator Model:

- Assumption 1: Average model based on instantaneous power balance equation.

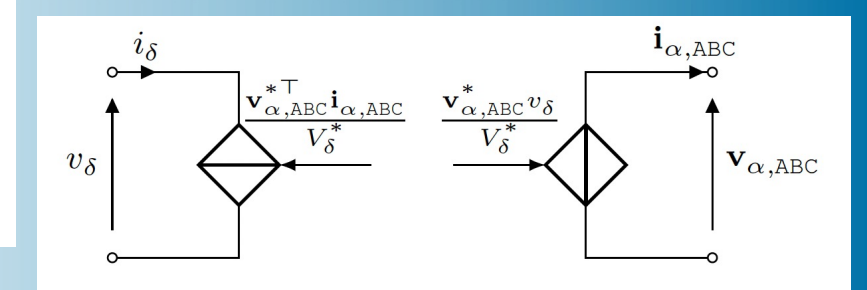
➤ Controlled current source on the DC side and controlled voltage source on the AC side.

➤ Linearization around

$$\mathbf{y}_o(t) = \begin{bmatrix} \bar{\mathbf{v}}_{\alpha,ABC}^*(t) \\ \bar{\mathbf{i}}_{\alpha,ABC}(t) \\ \bar{v}_\delta(t) \end{bmatrix} :$$

- All quantities are time-periodic.

➤ Expression can be employed when deriving the LTP model of the power hardware.



$$P_\delta = P_\alpha$$

$$\mathbf{v}_{\alpha,ABC}(t) = \frac{1}{V_\delta^*} \mathbf{v}_{\alpha,ABC}^*(t) v_\delta(t)$$

$$i_\delta(t) = \frac{1}{V_\delta^*} \mathbf{v}_{\alpha,ABC}^{*\top}(t) \mathbf{i}_{\alpha,ABC}(t)$$

$$\mathbf{v}_{\alpha,ABC}(t) \approx \frac{1}{V_\delta^*} \left(\bar{\mathbf{v}}_{\alpha,ABC}^*(t) v_\delta(t) + \bar{v}_\delta(t) \mathbf{v}_{\alpha,ABC}^*(t) - \bar{\mathbf{v}}_{\alpha,ABC}^*(t) \bar{v}_\delta(t) \right)$$

$$i_\delta(t) \approx \frac{1}{V_\delta^*} \left(\bar{\mathbf{v}}_{\alpha,ABC}^{*\top}(t) \mathbf{i}_{\alpha,ABC}(t) + \bar{\mathbf{i}}_{\alpha,ABC}^T(t) \mathbf{v}_{\alpha,ABC}^*(t) - \bar{\mathbf{i}}_{\alpha,ABC}^T(t) \bar{\mathbf{v}}_{\alpha,ABC}^*(t) \right)$$

Grid-Following CIDER – PWM_LCL_C_PI_VQ_I

Actuator Model:

- Assuring power

$$\hat{\mathbf{A}}_\pi = \begin{bmatrix} \ddots & \ddots & & & \\ & \mathbf{A}_{\pi,0} & \mathbf{A}_{\pi,-1} & & \\ & \mathbf{A}_{\pi,1} & \mathbf{A}_{\pi,0} & \mathbf{A}_{\pi,-1} & \\ & & \mathbf{A}_{\pi,1} & \mathbf{A}_{\pi,0} & \ddots \\ & & & \ddots & \ddots \end{bmatrix},$$

$$\text{with } \mathbf{A}_{\pi,h} = \frac{1}{V_\delta^*} \begin{bmatrix} \mathbf{0}_{3 \times 3} & \mathbf{0}_{3 \times 6} & \mathbf{L}_\alpha^{-1} \bar{\mathbf{V}}_{\alpha,ABC,h}^* \\ \mathbf{0}_{6 \times 3} & \mathbf{0}_{6 \times 6} & \mathbf{0}_{6 \times 1} \\ -C_\delta^{-1} \bar{\mathbf{V}}_{\alpha,ABC,h}^{*T} & \mathbf{0}_{1 \times 6} & 0 \end{bmatrix}$$

➤ Linearization around

$$\mathbf{y}_o(t) = \begin{bmatrix} \bar{\mathbf{v}}_{\alpha,ABC}^*(t) \\ \bar{\mathbf{i}}_{\alpha,ABC}(t) \\ \bar{v}_\delta(t) \end{bmatrix}:$$

- All quantities are linear time-periodic.

➤ Expression can be employed when deriving the LTP model of the power hardware.

The matrices of the power hardware model are no longer constant, but might exhibit nonzero Fourier coefficients at all harmonics.

- Matrices in harmonic domain will no longer exhibit a block-diagonal structure.
- There will be a stronger coupling between harmonics of different orders.

$$\begin{aligned} v_\delta(t) &= \frac{1}{V_\delta^*} \mathbf{v}_{\alpha,ABC}^*(t) v_\delta(t) \\ i_\delta(t) &= \frac{1}{V_\delta^*} \mathbf{v}_{\alpha,ABC}^{*T}(t) \mathbf{i}_{\alpha,ABC}(t) \end{aligned}$$

$$\mathbf{v}_{\alpha,ABC}(t) \approx \frac{1}{V_\delta^*} \left(\bar{\mathbf{v}}_{\alpha,ABC}^*(t) + \bar{v}_\delta(t) \mathbf{v}_{\alpha,ABC}^*(t) - \bar{\mathbf{v}}_{\alpha,ABC}^*(t) \bar{v}_\delta(t) \right)$$

$$i_\delta(t) \approx \frac{1}{V_\delta^*} \left(\bar{\mathbf{i}}_{\alpha,ABC}^{*T}(t) \mathbf{i}_{\alpha,ABC}(t) + \bar{\mathbf{i}}_{\alpha,ABC}^{*T}(t) \mathbf{v}_{\alpha,ABC}^*(t) - \bar{\mathbf{i}}_{\alpha,ABC}^{*T}(t) \bar{\mathbf{v}}_{\alpha,ABC}^*(t) \right)$$

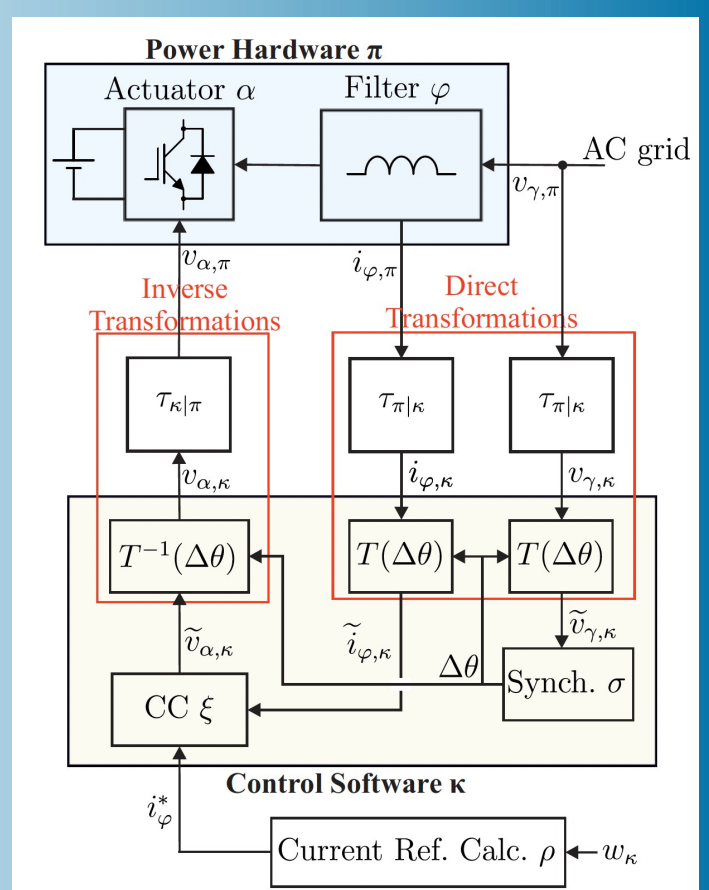
Grid-Following CIDER – PWM_LCL_PI_PQ_PLL

Further explanations and detailed derivation in [19].

- Power hardware consists of:
 - AC filter stages.¹
- Transformations.
- Control software:
 - AC controller stages.¹
 - PLL + parts of the transformations.
- Reference calculation.¹

Nonlinearities within the internal response of the CIDER.
→ Linearization in time domain around time-periodic trajectories.

¹Same procedure as for PWM_LCL_PI_PQ

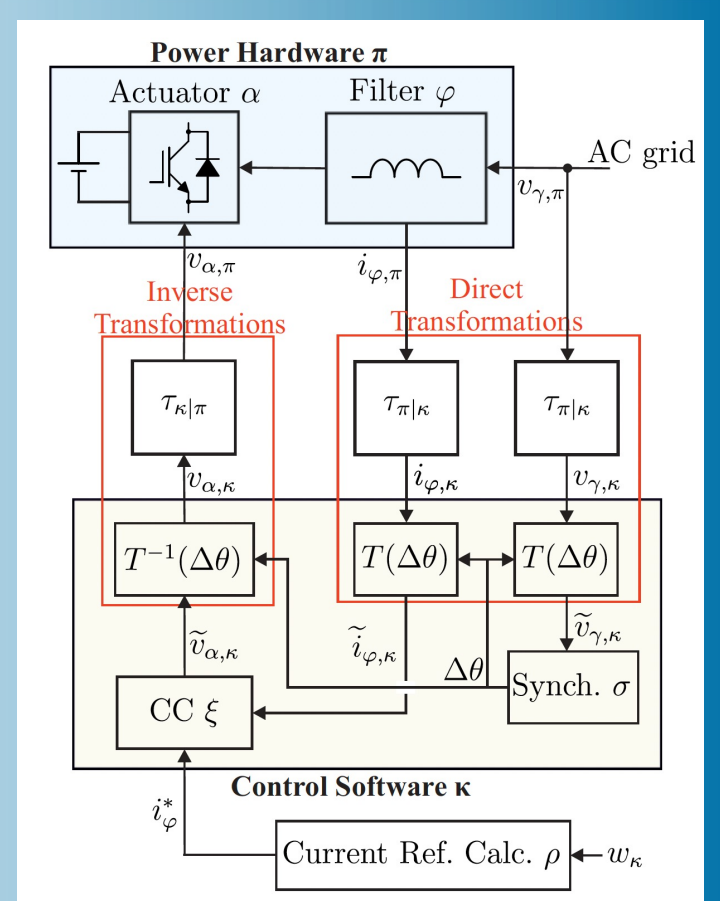


Grid-Following CIDER – PWM_LCL_PI_PQ_PLL

- Modelling of the synchronization (SRF-PLL) as an LTI system.
- Transformation matrices with time-periodic $\theta(t)$:
 - $\tilde{\theta}(t) = \theta(t) + \Delta\theta(t)$, with $\Delta\theta(t)$ being a zero-average periodic signal.
 - $\Delta\theta(t)$ is responsible for an additional rotation of the transformed signals in DQ frame:

$$T(\Delta\theta(t)) = \begin{bmatrix} \cos(\Delta\theta(t)) & \sin(\Delta\theta(t)) \\ -\sin(\Delta\theta(t)) & \cos(\Delta\theta(t)) \end{bmatrix} \approx \begin{bmatrix} 1 & \Delta\theta(t) \\ -\Delta\theta(t) & 1 \end{bmatrix}$$

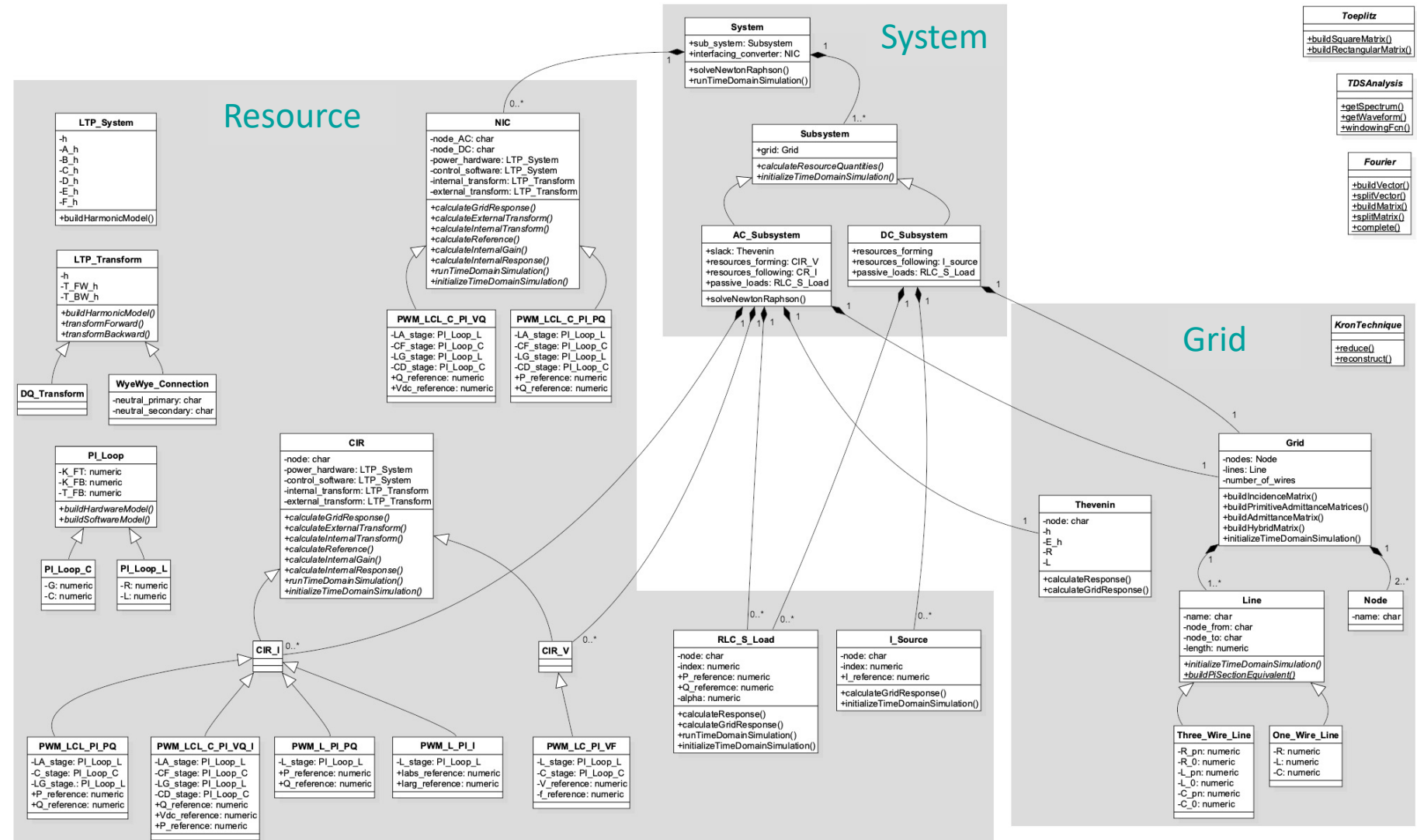
- Further linearizations of the products of state variables (i.e., the measured signals $\tilde{i}_{\varphi,DQ}(t)$, etc and $\Delta\theta(t)$ are handled as shown before.



Matlab Code:

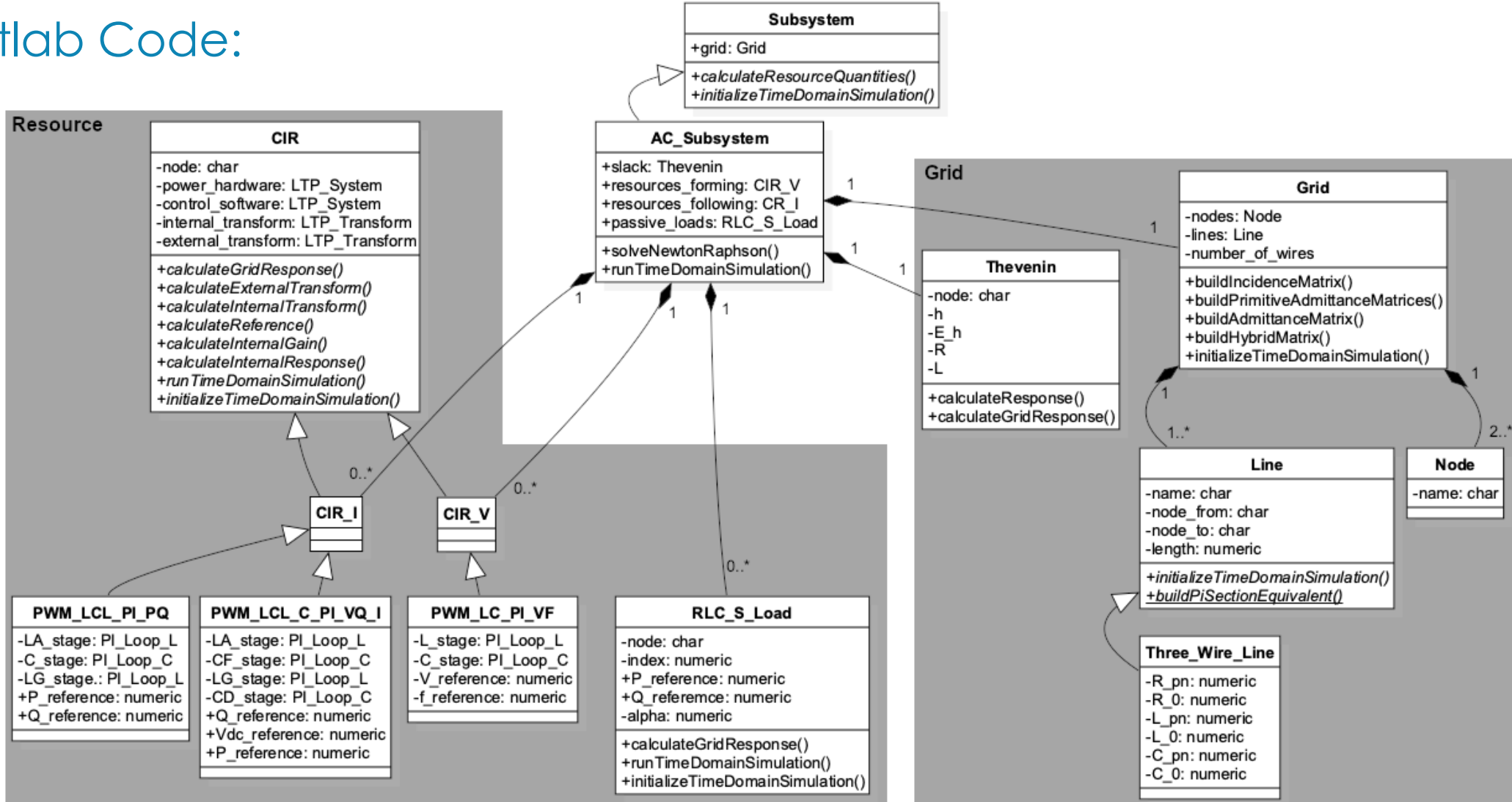
The Code provided on Github includes the functionalities for an extension of the HPF to analyse AC/DC hybrid grids [20].

→ For what is discussed in this Tutorial only a subsection of this UML diagram is relevant (see next slide).



Complete UML diagram for the HPF code.

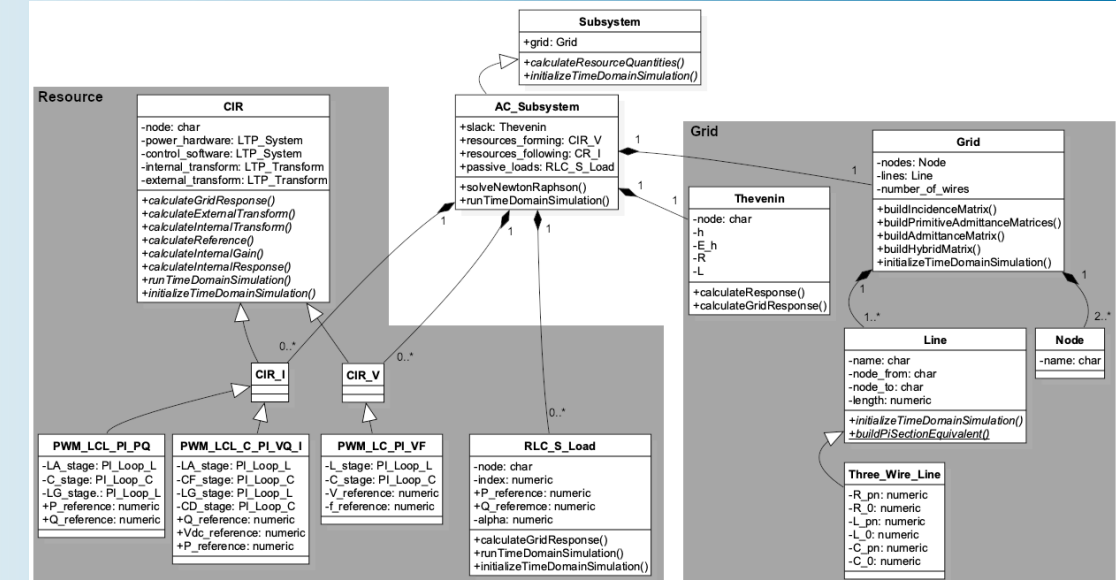
Matlab Code:



Subsection of the UML diagram for the HPF code.

Matlab Code:

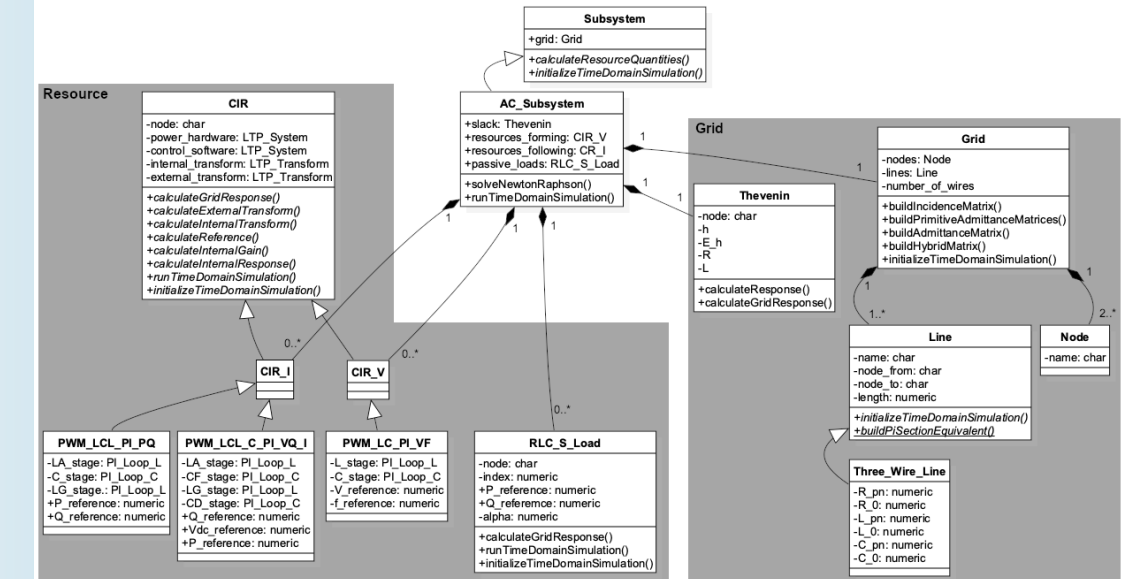
- Project follows the philosophy of Object-Oriented Programming (OOP) → Structure allows to easily scale the project.
- Like the framework of the HPF, the code has two main parts (i.e., classes related to the resources and the grid).
- All objects are built from excel files that contain the fixed parameters.
- One can then run predefined functions on the individual objects.
- Resources:
 - Contain grid-forming and -following CIDERs, and passive impedance loads.
 - CIRs consist of power hardware, control software, internal and external transformation.
 - Any resource class possesses the function `calculateGridResponse()`.
- Grid:
 - Possesses the function `buildHybridMatrix()` needed in a Newton-Raphson iteration.



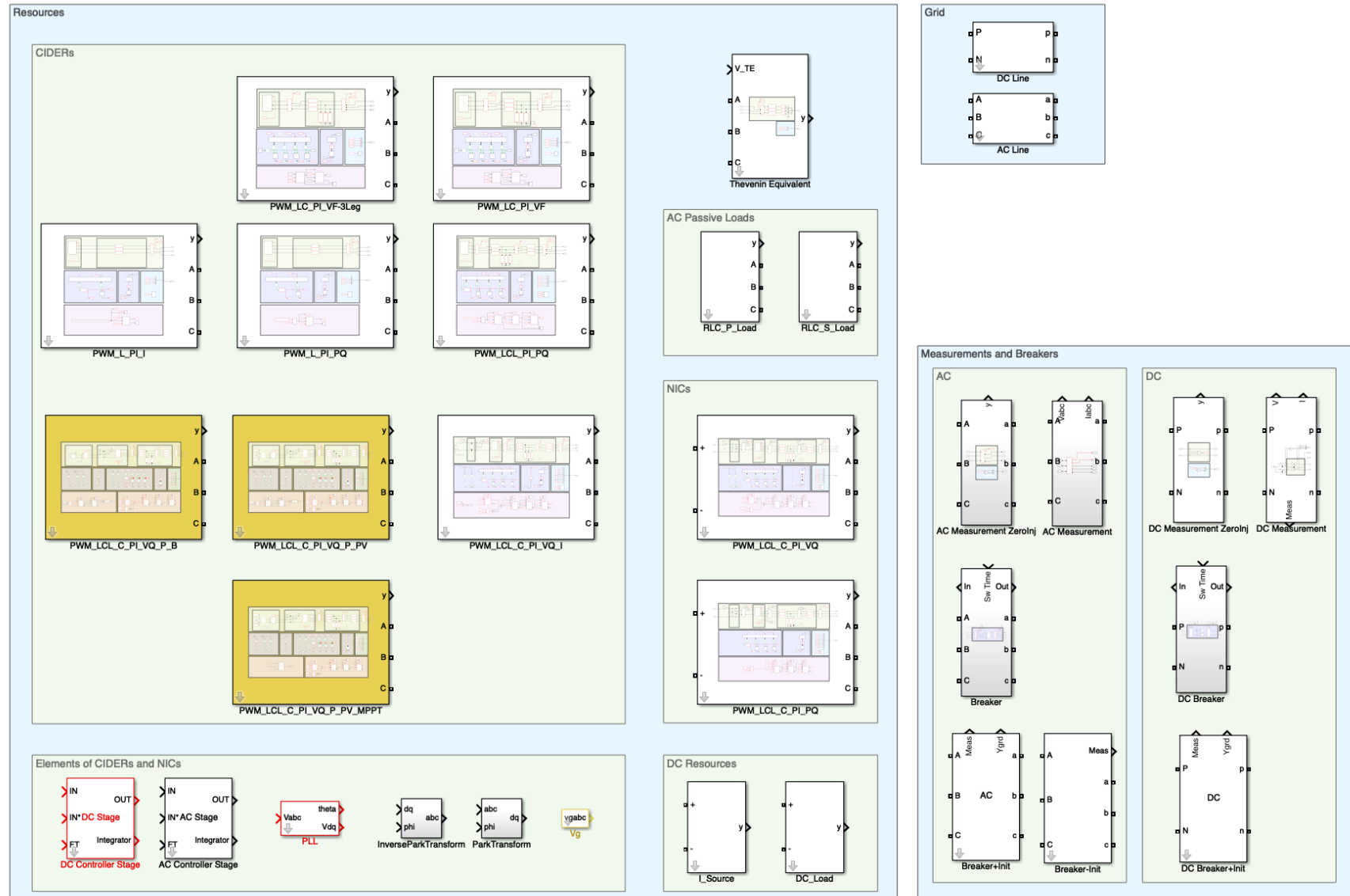
Matlab Code:

System:

- The HPF can be performed on an object of the class System.
- A system consists of:
 - One grid, composed of Nodes and Lines.
 - One slack node, namely a TE.
 - One or several objects of the class CIR_V (grid-forming CIDER).
 - One or several objects of the class CIR_I (grid-following CIDER).
 - One or several objects of the class RLC_S_Load (passive load).
- Calling `solveNewtonRaphson()` uses all these objects and their parameters/functions to perform the HPF study.



Simulink Library:



Simulink:

- HPF study is validated using Time-Domain Simulations performed with Simulink.
- The Simulink Library includes all available models of CIDERs, plus commonly used elements of power systems (lines, measurement blocks, passive loads, etc.)
- Can be used to plug together the power system for validation purposes.
- The parameters of the components of the Simulink models are automatically initialized from the previously introduced Matlab objects (i.e., through their `obj.initializeTimeDomainSimulation()`).

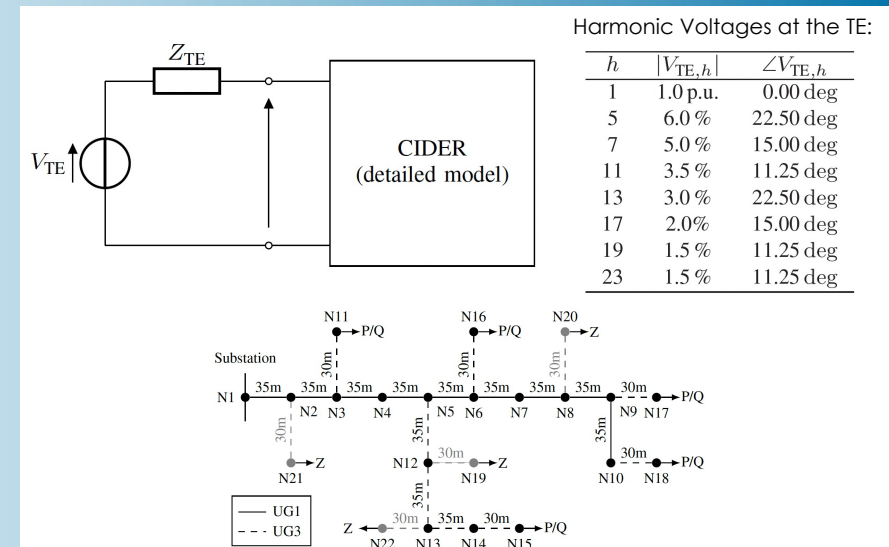


Overview – Resource and System Validation

- Individual CIDERs and the HPF algorithm are validated through Time-Domain Simulations (TDS) with Simulink.

Today:

- Resource: Grid response of the CIDER including the DC side (PWM_LCL_C_PI_VQ_I).
- Algorithm of entire systems – here: 4Bus system.
 ➤ Demonstration in Matlab.



The validation of other resources and systems can be found in the corresponding papers [12,18,19].

Resource Validation - CIDER including DC Side (PWM_LCL_C_PI_VQ_I)

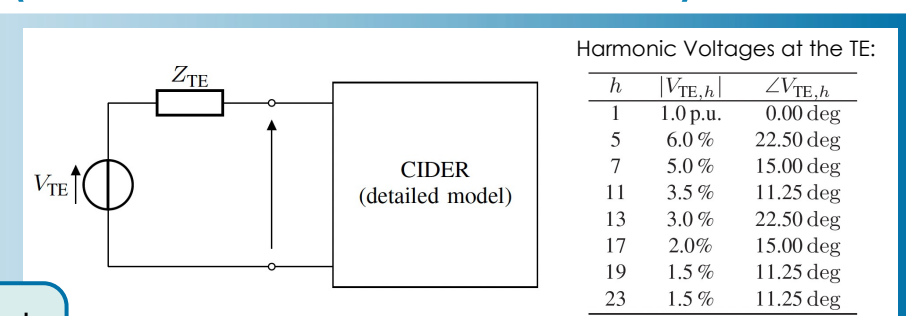
- Time-Domain Simulations (TDS) with Simulink:
 - DFT of 5 periods of the steady-state waveforms.
 - Thévenin Equivalent (TE) injects a specified level of harmonics.

Further details can be found in [18].

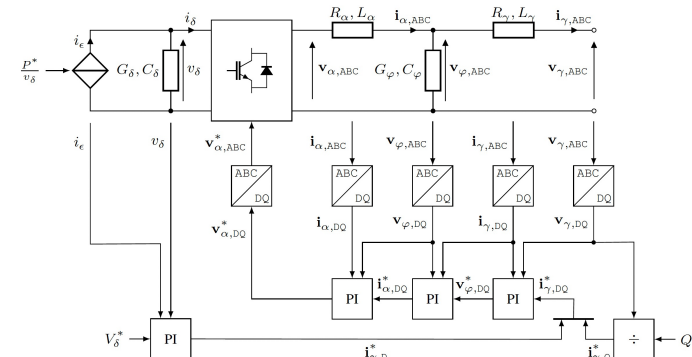
Procedure:

- Spectrum of the input quantity for the grid response is taken from TDS: $\hat{\mathbf{W}}_\gamma = \hat{\mathbf{V}}_{\gamma,\text{TDS}}$.
- Spectrum of the operating point $\hat{\mathbf{Y}}_o$ is also taken from TDS.
- Output from the grid response $\hat{\mathbf{Y}}_\gamma = \hat{\mathbf{I}}_{\gamma,\text{HPF}}$ is then compared to the spectrum of the TDS $\hat{\mathbf{I}}_{\gamma,\text{TDS}}$.

- Allows to do a preliminary check of the accuracy of the resources' grid responses.



Structure of the CIDER including the DC side [18]:

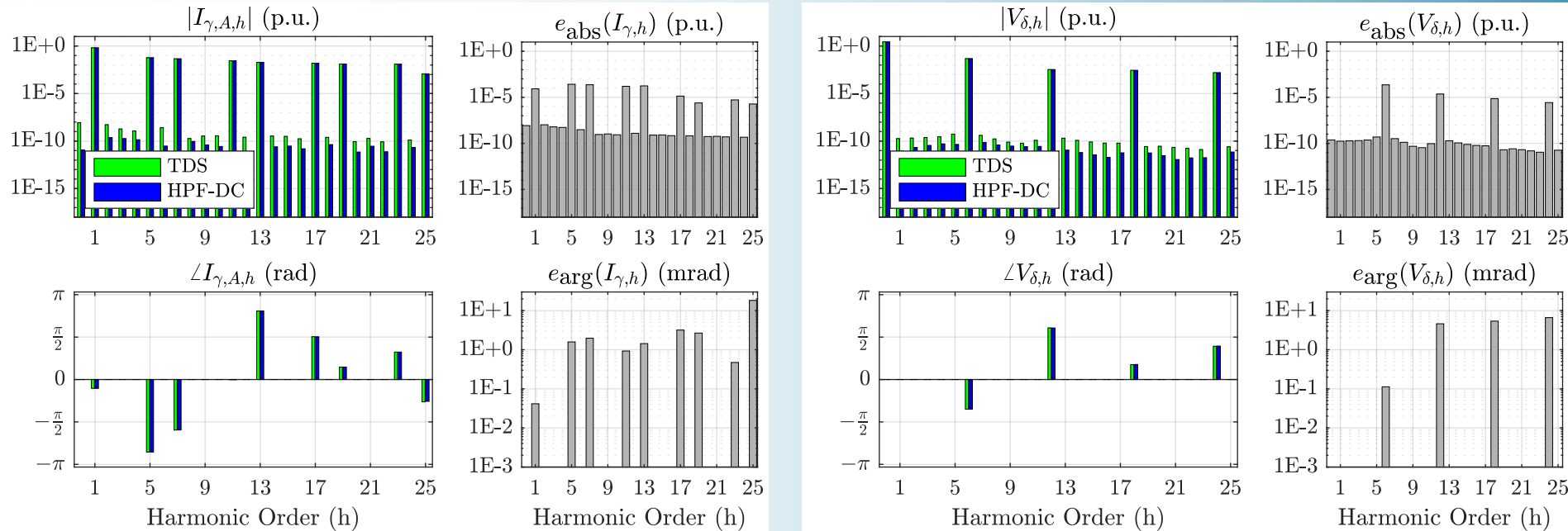
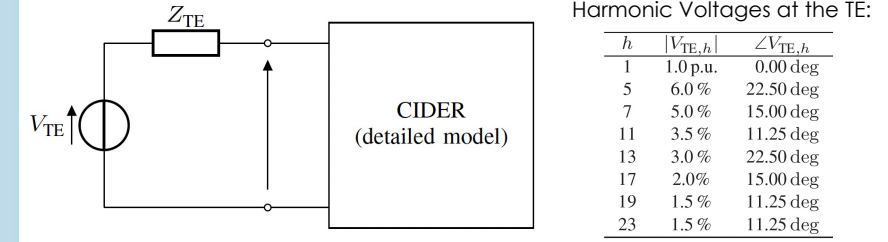


Parameters of the CIDER (rated power 60kVA) [18]:

Filter stage	L/C	R/G	K_{FB}	T_{FB}	K_{FT}
DC-Link Capacitor (δ)	310 μF	0 S	10	3e-3	1
Actuator-side inductor (α)	325 μH	1.02 m Ω	9.56	1.47e-4	1
Capacitor (φ)	90.3 μF	0 S	0.569	8.97e-4	0
Grid-side inductor (γ)	325 μH	1.02 m Ω	0.23	1e-3	1

Resource Validation - CIDER including DC Side (PWM_LCL_C_PI_VQ_I)

- Magnitude and phase of the CIDER's controlled quantities are compared between the HPF and TDS:
 - Phase A of the grid current \hat{I}_γ .
 - The DC voltage \hat{V}_δ .
- The error plots describe the maximum absolute errors over all phases in magnitude and phase, respectively.



Grid current and DC-side voltage of a grid-following CIDER including the DC-side modelling.

System Validation – 4Bus System

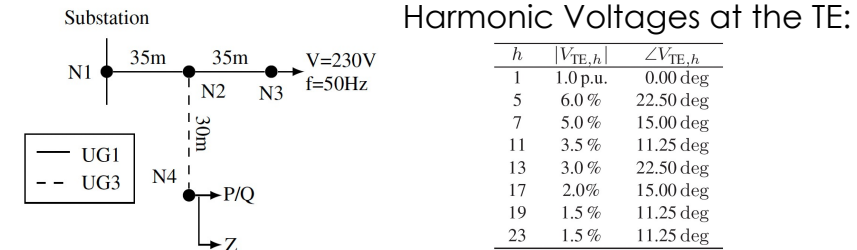
- Time-Domain Simulations (TDS) with Simulink:
 - DFT of 5 periods of the steady-state waveforms.
 - Substation injects a specified level of harmonics.
- Initialization of the algorithm: values of AC and DC quantities are based on balanced, sinusoidal conditions and nominal values or reference setpoints

Details concerning the parameters of the CIDERs can be found in the excel files contained in the Git repository and in [12].

Tutorial slides and code available on:



<https://github.com/DESL-EPFL/Harmonic-Power-Flow-Method>



Sequence parameters of the lines:

ID	R_+/R_-	R_0	L_+/L_-	L_0	C_+/C_-	C_0
UG1	0.162 Ω	0.529 Ω	0.262 mH	1.185 mH	637 nF	388 nF
UG3	0.822 Ω	1.794 Ω	0.270 mH	3.895 mH	637 nF	388 nF

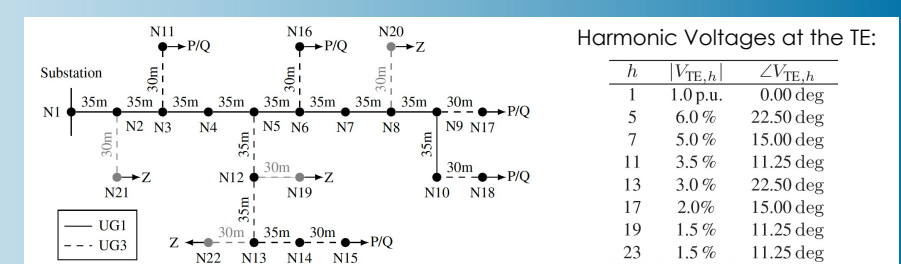
Setpoints of the CIDERs and Loads in the system:

Node	P	Q	Phase weights	Type
N04-1	-47.5 kW	-15.6 kVAr	[0.33 0.33 0.33]	P/Q (constant-power)
N04-2	-33.4 kW	-10.9 kVAr	[0.31 0.50 0.19]	Z (constant-impedance)

System Validation – 22Bus System from [18]

- Time-Domain Simulations (TDS) with Simulink:
 - DFT of 5 periods of the steady-state waveforms.
 - Substation injects a specified level of harmonics.
 - Initialization of the algorithm: values of AC and DC quantities are based on balanced, sinusoidal conditions and nominal values or reference setpoints

Further details can be found in [18].



Harmonic Voltages at the TE:		
h	$ V_{\text{TE},h} $	$\angle V_{\text{TE},h}$
1	1.0 p.u.	0.00 deg
5	6.0 %	22.50 deg
7	5.0 %	15.00 deg
11	3.5 %	11.25 deg
13	3.0 %	22.50 deg
17	2.0%	15.00 deg
19	1.5 %	11.25 deg
23	1.5 %	11.25 deg

Parameters of the CIDERs and Loads in the system [18]:

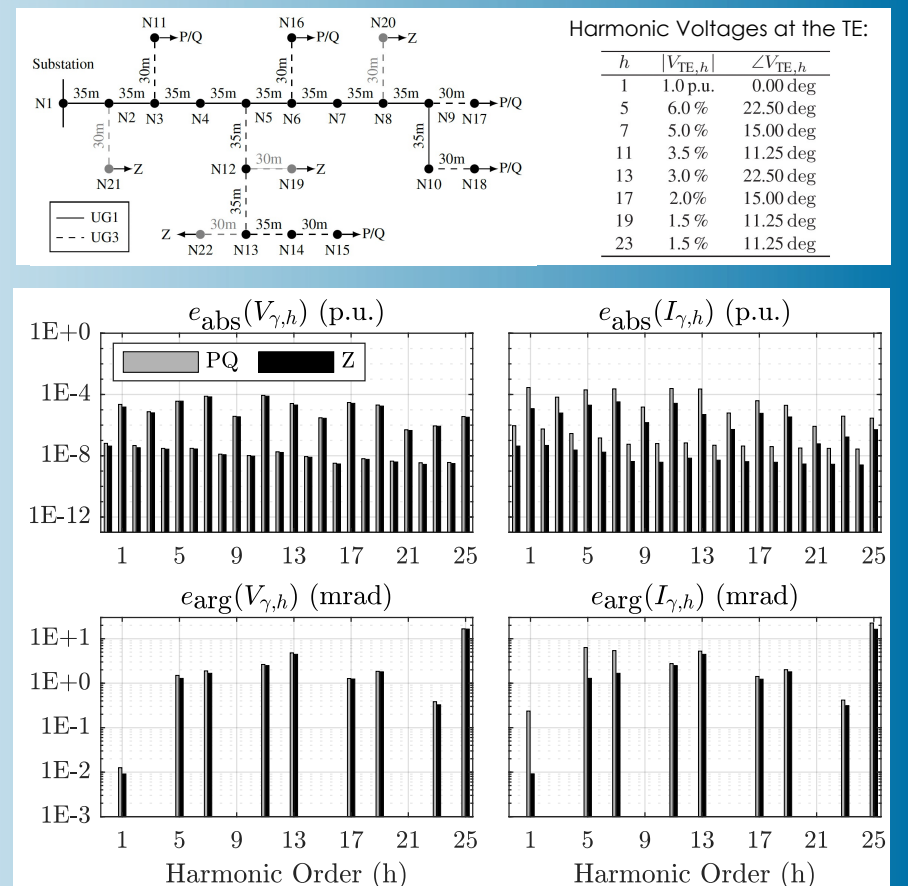
Node	S	pf	Type	Phase weights
N11	15.0 kW	0.95	P/Q	[0.33 0.33 0.33]
N15	52.0 kW	0.95	P/Q	[0.33 0.33 0.33]
N16	55.0 kW	0.95	P/Q	[0.33 0.33 0.33]
N17	35.0 kW	0.95	P/Q	[0.33 0.33 0.33]
N18	47.0 kW	0.95	P/Q	[0.33 0.33 0.33]
N19	-51.2 kW	0.95	Z	[0.31 0.50 0.19]
N20	-51.7 kW	0.95	Z	[0.45 0.23 0.32]
N21	-61.5 kW	0.95	Z	[0.24 0.39 0.37]
N22	-61.9 kW	0.95	Z	[0.31 0.56 0.13]

Parameters of the CIDERs (rated power 60kVA) [18]:

Filter stage	L/C	R/G	K_{FB}	T_{FB}	K_{FT}
DC-Link Capacitor (δ)	310 μF	0 S	10	3e-3	1
Actuator-side inductor (α)	325 μH	1.02 m Ω	9.56	1.47e-4	1
Capacitor (φ)	90.3 μF	0 S	0.569	8.97e-4	0
Grid-side inductor (γ)	325 μH	1.02 m Ω	0.23	1e-3	1

System Validation – 22Bus System from [18]

- The nodal quantities at the nodes with CIDERs and passive impedance loads are compared between HPF and TDS.
 - The plots show the maximum absolute errors over all nodes and phases, for voltages (left column) and currents (right column), in magnitude (top row) and phase (bottom row).
- HPF algorithm accurately analyses the propagation of harmonics.



Results of the validation on the benchmark system for the grid-following CIDERs (PQ) and the constant impedance loads (Z).

Further Studies using the HPF:

1. Comparison of the proposed HPF method with a decoupled HPF.
→ Details in [18].
2. Comparison of the proposed HPF method when ex- or including the DC side of CIDERS.
→ Details in [18].
3. Harmonic coupling in grids with PLL synchronized CIDERS - Analysis of a highly loaded system with distorted grid supply voltage.
→ Details in [19].

Upcoming at PowerTech 2023:

- Presentation of [19] (Paper 131, "LTP Modeling and Analysis of Frequency Coupling in PLL-Synchronized Converters for Harmonic Power Flow Studies"):
Monday, 26th June, 15:30-17:00 in S3 - Dynamics of converter-based power systems.
- Presentation of [20] (Paper 146, "Harmonic power-flow study of hybrid AC/DC grids with converter-interfaced distributed energy resources"):
Thursday, 29th June, 15:30-17:00 in S31 - Load flow and power quality.

- [1] Farrokhabadi, Mostafa, et al. "Microgrid stability definitions analysis and modeling." *IEEE Power Energy Soc., Piscataway, NJ, USA, Tech. Rep. PES-TR66* (2018).
- [2] A. G. Phadke and J. H. Harlow, "Generation of abnormal harmonics in high-voltage AC/DC power systems", *IEEE Trans. Power App. Syst.*, vol. 87, no. 3, pp. 873–883, Mar. 1968.
- [3] J. H. R. Enslin and P. J. M. Heskes, "Harmonic interaction between a large number of distributed power inverters and the distribution network", *IEEE Trans. Power Electron.*, vol. 19, no. 6, pp. 1586–1593, Nov. 2004.
- [4] H. W. Dommel, "Digital computer solution of electromagnetic transients in single- and multiphase networks," *IEEE Trans. Power App. Syst.*, no. 4, pp. 388–399, 1969.
- [5] L. W. Nagel and D. O. Pederson, "SPICE: Simulation program with integrated circuit emphasis," UC Berkeley, Tech. Rep. UCB M382, 1973.
- [6] J. Mahseredjian et al., "On a new approach for the simulation of transients in power systems," *Elect. Power Syst. Research*, vol. 77, no. 11, pp. 1514–1520, 2007.
- [7] J. Arriaga et al., *Power System Harmonic Analysis*. Hoboken, NJ, USA: Wiley, 1997.
- [8] S. Herraiz et al., "Review of harmonic load-flow formulations," *IEEE Trans. Power Del.*, vol. 18, no. 3, pp. 1079–1087, 2003.
- [9] A. Semlyen and A. Medina, "Computation of the periodic steady-state in systems with nonlinear components using a hybrid time- and frequency domain methodology," *IEEE Trans. Power Syst.*, vol. 10, no. 3, pp. 1498–1504, 1995.
- [10] W. Wiechowski et al., "Hybrid time/frequency-domain modelling of nonlinear components," in *Proc. Int. Conf. Elect. Power Qual. Util.*, Barcelona, CAT, ES, 2007, pp. 1–6.
- [11] A. M. Kettner, L. Reyes-Chamorro, J. K. Maria Becker, Z. Zou, M. Liserre and M. Paolone, "Harmonic Power-Flow Study of Polyphase Grids With Converter-Interfaced Distributed Energy Resources—Part I: Modeling Framework and Algorithm," in *IEEE Transactions on Smart Grid*, vol. 13, no. 1, pp. 458–469, Jan. 2022, doi: 10.1109/TSG.2021.3120108.
- [12] J. K. M. Becker, A. M. Kettner, L. Reyes-Chamorro, Z. Zou, M. Liserre and M. Paolone, "Harmonic Power-Flow Study of Polyphase Grids With Converter-Interfaced Distributed Energy Resources—Part II: Model Library and Validation," in *IEEE Transactions on Smart Grid*, vol. 13, no. 1, pp. 470–481, Jan. 2022, doi: 10.1109/TSG.2021.3120081.
- [13] N. M. Wereley, "Analysis and control of linear periodically time-varying systems," Ph.D. dissertation, MIT, Cambridge, MA, USA, 1991.
- [14] X. Wang and F. Blaabjerg, "Harmonic stability in power-electronic-based power systems: Concept, modeling, and analysis," *IEEE Trans. Smart Grid*, vol. 10, no. 3, pp. 2858–2870, 2019.
- [15] J. B. Kwon et al., "Harmonic interaction analysis in a grid-connected converter using harmonic state-space modeling," *IEEE Trans. Power Electron.*, vol. 32, no. 9, pp. 6823–6835, 2016.
- [16] M. Paolone, et al. "Fundamentals of power systems modelling in the presence of converter-interfaced generation." *Electric Power Systems Research* 189 (2020): 106811.
- [17] J. Rocabert, A. Luna, F. Blaabjerg and P. Rodríguez, "Control of Power Converters in AC Microgrids," in *IEEE Transactions on Power Electronics*, vol. 27, no. 11, pp. 4734–4749, Nov. 2012, doi: 10.1109/TPEL.2012.2199334.
- [18] J. K. M. Becker et al., "Modelling of AC/DC Interactions of Converter-Interfaced Resources for Harmonic Power-Flow Studies in Microgrids," in *IEEE Transactions on Smart Grid*, vol. 14, no. 3, pp. 2096–2110, May 2023, doi: 10.1109/TSG.2022.3216910.
- [19] F. Cecati, J. K. M. Becker, S. Pugliese, Y. Zuo, M. Liserre and M. Paolone, "LTP Modeling and Analysis of Frequency Coupling in PLL-Synchronized Converters for Harmonic Power Flow Studies," in *IEEE Transactions on Smart Grid*, doi: 10.1109/TSG.2022.3228616.
- [20] J. K. M. Becker, A. M. Kettner, Y. Zuo, and M. Paolone, "Harmonic power-flow study of hybrid ac/dc grids with converter-interfaced distributed energy resources," arXiv, 2023. doi: 10.48550/ARXIV.2302.02864. [Online]. Available: <https://arxiv.org/abs/2302.02864>.



IEEE
Power & Energy Society

IEEE

PowerTech
Belgrade 2023

LEADING INNOVATIONS FOR RESILIENT
& CARBON-NEUTRAL POWER SYSTEMS
25-29 JUNE, 2023, BELGRADE, SERBIA

THANK YOU FOR YOUR ATTENTION!



Contact Information:

Johanna Becker
École Polytechnique Fédérale Lausanne
Johanna.becker@epfl.ch



LEADING INNOVATIONS FOR RESILIENT
& CARBON-NEUTRAL POWER SYSTEMS
25-29 JUNE, 2023, BELGRADE, SERBIA